MONTANA STATE UNIVERSITY

Analytical investigation of the vibrational behavior of earth dams
by Gerald Alvin Frazier

A thesis submitted to the Graduate Faculty in partial fulfillment of the requirements for the degree of
MASTER OF SCIENCE in Civil Engineering
Montana State University
© Copyright by Gerald Alvin Frazier (1966)

Abstract:
A method is presented for calculating the natural frequencies of vibration and the corresponding mode shapes of an earth dam. The dam is treated as an elastic two-dimensional shear-wedge having arbitrary boundaries which are fashioned to simulate the irregular foundation and abutments of a dam. A method is also presented for calculating the general response of an earth dam to arbitrary motion of the boundaries by superimposing the response of each mode.

The natural frequencies and mode shapes of a full scale dam are calculated and compared with the natural frequencies and mode shapes obtained from vibration tests on the dam. The first six computed natural frequencies are consistently higher than the observed frequencies by amounts varying from 11% to 25%. The general shape of the first four computed modes shows good agreement with the observed modes along the crest of the dam but poor agreement in the lower regions of the dam. The computed deflections are much larger than the measured deflections in the lower regions. This discrepancy is attributed to the presence of strains through the thickness of the dam which were ignored in the analytical investigation.

ANALYTICAL INVESTIGATION OF THE VIBRATIONAL BEHAVIOR OF EARTH DAMS

by

Gerald A. Frazier

A thesis submitted to the Graduate Faculty in partial fulfillment of the requirements for the degree

of

MASTER OF SCIENCE

in

Civil Engineering

Approved:

Head, Major Department

Chairman, Examining Committee

Graduate Dean

MONTANA STATE UNIVERSITY
Bozeman, Montana

June, 1966

ACKNOWLEDGMENTS

The author wishes to express his appreciation to all those individuals who offered their personal assistance and helped to make this investigation possible. The author wishes to express his sincere thanks to one individual in particular who assisted in all phases of this investigation. Dr. W. O. Keightley gave freely of both his time and his valuable advice, and by his interest in the work, he served as a great source of encouragement.

Dr. Glen Ingram and the computing center staff at Montana State University offered their assistance with computing problems that arose, and the author is grateful. Many individuals at Lawrence Radiation Laboratory, Livermore, California, offered their technical assistance. The author is particularly thankful to John Korver and Dr. Joe Knox for their assistance with the work.

The final draft of this thesis and all of the many rough drafts were typed by Mrs. Gerald A. Frazier, the author's wife. She has shown forbearance and understanding throughout the entire study, and the author is both grateful and indebted to her.

Most of the digital computer work and a portion of the author's support was provided for by National Science Foundation Grant GP-2444, to investigate the application of the

Holzer Method for finding the natural frequencies of two-dimensional shear structures, under the direction of Professor W. O. Keightley. The major portion of the author's support during the tenure of this study was provided by a National Science Foundation Traineeship awarded by the College of Engineering at Montana State University. The author was also employed by Lawrence Radiation Laboratory for one summer, where computing facilities were provided for continuing the investigation of the vibrational behavior of earth dams.

TABLE OF CONTENTS

Chapter I INTRODUCTION 1

Chapter II MATHEMATICAL REPRESENTATION OF AN EARTH DAM 2

Methods of Approach 2

Mathematical Model of an Earth Dam 10

Chapter III CALCULATING DYNAMIC BEHAVIOR 13

Calculating Natural Frequencies and Mode Shapes 13

General Response Due to Arbitrary Boundary Motion 23

Chapter IV CALCULATED BEHAVIOR 38

Computer Code 38

Mathematical Check on Natural Frequencies and Mode Shapes 39

Dynamic Behavior of Bouquet Dam 47

Chapter V SUMMARY AND CONCLUSIONS 65

Summary 65

Conclusions 68

Chapter VI RECOMMENDATIONS FOR FUTURE WORK 72

Refinements of the Model 72

TABLE OF CONTENTS (Cont.)

APPENDIX 78

A. Differential Equation of Motion for a Shear Dam 79

B. Orthogonality of the Modes of Vibration of a Shear Dam 82

C. Proposed Verification of Mode Superposition Calculations 85

LITERATURE CITED 89

LIST OF TABLES

TABLE I — Comparison of the Natural Frequencies Obtained by a Finite-Element Approximation with the Exact Natural Frequencies for a Truncated Shear-Wedge 46

TABLE II — Observed and Computed Natural Frequencies of Bouquet Dam 54

LIST OF FIGURES

Figure		
1	Infinitesimal Element of Material	4
2	Discrete Approximation of a Shear Dam	14
3	Block of Earth Represented by a Point Mass	15
4	Mass-Spring Grid Illustrating the Step-by-Step Procedure for Calculating Internal Shears and Deflections	20
5	Plan View of an Earth Dam Showing Seismic Waves at an Oblique Angle	25
6	Single Degree of Freedom System	33
7	Truncated Shear-Wedge	43
8	First Three Horizontal Mode Shapes of a Truncated Shear-Wedge	48
9	First Three Vertical Mode Shapes of a Truncated Shear-Wedge	49
10	Cross-Section of Bouquet Canyon Dam	51
11	Elevation View of Bouquet Canyon Dam Showing Finite-Element Approximation	52
12	Cross-Section and Elevation View of Bouquet Dam Showing Truncated Shear-Wedge Approximatiom	56
13	Computed Mode Shapes Compared with Observed Mode Shapes	60
14	Infinitesimal Element of Soil Extending Through the Dam	80

ABSTRACT

A method is presented for calculating the natural frequencies of vibration and the corresponding mode shapes of an earth dam. The dam is treated as an elastic two-dimensional shear-wedge having arbitrary boundaries which are fashioned to simulate the irregular foundation and abutments of a dam. A method is also presented for calculating the general response of an earth dam to arbitrary motion of the boundaries by superimposing the response of each mode.

The natural frequencies and mode shapes of a full scale dam are calculated and compared with the natural frequencies and mode shapes obtained from vibration tests on the dam. The first six computed natural frequencies are consistently higher than the observed frequencies by amounts varying from 11% to 25%. The general shape of the first four computed modes shows good agreement with the observed modes along the crest of the dam but poor agreement in the lower regions of the dam. The computed deflections are much larger than the measured deflections in the lower regions. This discrepancy is attributed to the presence of strains through the thickness of the dam which were ignored in the analytical investigation.

Chapter I

INTRODUCTION

Earth dams are a common feature in today's industrialized society. The extensive services rendered are often irreplaceable, and the potential destructuve power of a catastrophic failure can be enormous. Like many other structures, dams are susceptible to failures which are caused by the shaking motion of the underlying foundations resulting from an earthquake or a large explosion. The need for understanding the behavior of dams for the purpose of economically designing safe, functional dams is apparent.

Each year better relationships between seismic motion and the resulting behavior of a dam are being established. The growing body of knowledge about the phenomonon governing the behavior of dams is made up of contributions by many research engineers. Results of both experimental and analytical investigations contribute to this growing body of knowledge. The purpose of this investigation is to present an analytical method for calculating some of the major features of the vibrational behavior of an earth dam.

Chapter II

MATHEMATICAL REPRESENTATION OF AN EARTH DAM

Methods of Approach

A method which is applicable in one way or another to nearly all engineering problems is the empirical method. This method attempts to predict an event on the basis of the observed behavior of similar events. The empirical method was used for the design of earth dams long before other more rational methods were available. An example of the method used in its crudest form migh be as follows. If a particular dam fails, then certainly a stronger design should be used on all similar dams. The empirical method in a more sophisticated form can be used to predict structural damage provided sufficient data of similar events are available and the effects of each governing parameter are well understood. The lack of experimental data plus the unique problems associated with each dam limits the use of this method considerably as a design tool.

As a first approximation to the stresses in the dam caused by ground motion, the dam and its foundation might be considered to be completely rigid. The acceleration at each point in the dam would then be the same as that of the foundation, and the force transmitted from the foundation to the dam would be the product of the mass of the dam and acceler-

ation of the foundation. The shear force at any height in the dam would be the product of the mass above the level of the force and the acceleration of the foundation, and the shear stress at any height could then be calculated from the shear force at that height. This approximation is not very representative of the actual behavior of a dam because neither completely rigid dams nor completely rigid foundations exist in reality, and the accelerations in an actual dam depend not only on the ground motion but also on the vibrational properties of the dam and its foundation.

A more rational approach to the problem is to consider that a dam responds to ground motion as a deformable body. The application of Newton's second law of motion to an infinitesimal element of the dam, shown in Figure 1, results in three general equations of motion:

$$\frac{\partial \sigma_{xx}}{\partial x} + \frac{\partial \sigma_{yx}}{\partial y} + \frac{\partial \sigma_{zx}}{\partial z} = \rho \frac{\partial^2 U}{\partial t^2}$$

$$\frac{\partial \sigma_{xy}}{\partial x} + \frac{\partial \sigma_{yy}}{\partial y} + \frac{\partial \sigma_{zy}}{\partial z} = \rho \frac{\partial^2 V}{\partial t^2}$$

$$\frac{\partial \sigma_{xz}}{\partial x} + \frac{\partial \sigma_{yz}}{\partial y} + \frac{\partial \sigma_{zz}}{\partial z} = \rho \frac{\partial^2 W}{\partial t^2} \quad \text{..... 1}$$

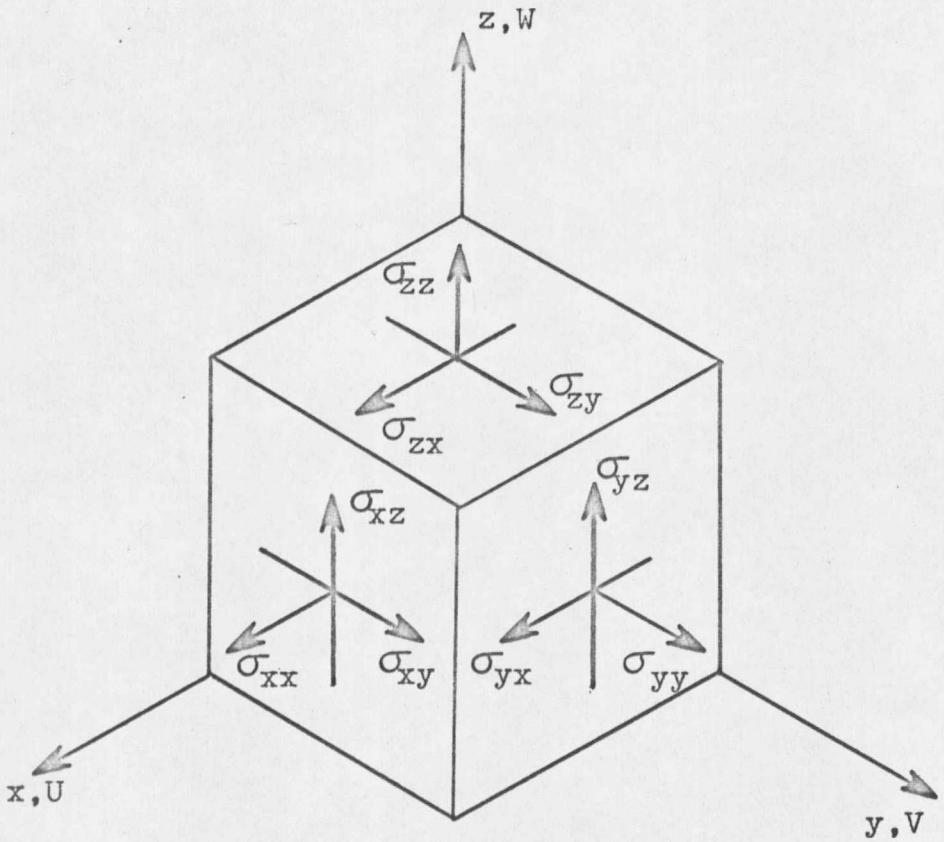


Figure 1: Infinitesimal Element of Material.

where the σ terms represent the stresses on the element of Figure 1, ρ is the mass density, and U, V, and W, are the displacements in the x, y, and z, direction respectively. The nine components of stress are reduced to six components by substituting:

$$\sigma_{xy} = \sigma_{yx}$$
$$\sigma_{xz} = \sigma_{zx}$$
$$\sigma_{yz} = \sigma_{zy}$$

as required for equilibrium of the element. The remaining six components of stress are related to strain by Hooke's law:

$$\frac{\partial U}{\partial x} = \frac{1}{E}\left[\sigma_{xx} - \nu\left(\sigma_{yy} + \sigma_{zz}\right)\right]$$
$$\frac{\partial V}{\partial y} = \frac{1}{E}\left[\sigma_{yy} - \nu\left(\sigma_{xx} + \sigma_{zz}\right)\right]$$
$$\frac{\partial W}{\partial z} = \frac{1}{E}\left[\sigma_{zz} - \nu\left(\sigma_{xx} + \sigma_{yy}\right)\right]$$
$$\frac{\partial U}{\partial y} + \frac{\partial V}{\partial x} = \frac{1}{G}\sigma_{xy}$$
$$\frac{\partial U}{\partial z} + \frac{\partial W}{\partial x} = \frac{1}{G}\sigma_{xz}$$
$$\frac{\partial V}{\partial z} + \frac{\partial W}{\partial y} = \frac{1}{G}\sigma_{yz} \qquad \text{.....} \qquad 2$$

where E is the modulus of elasticity, G is the modulus of rigidity, and ν is Poisson's ratio which relates E and G as follows:

$$E = 2\,(1+\nu)\,G\,.$$

The relationship between stress and strain, as expressed in equation (2), does not allow for dependency of E and G on the direction of orientation; therefore, at this point the assumption is made that the earth in a dam is isotropic.

Solving for stress in terms of strain and substituting into equation (1) gives a general form for the equation of motion in terms of displacement:

$$\frac{\partial}{\partial x}\left[\lambda e+2G\frac{\partial U}{\partial x}\right]+\frac{\partial}{\partial y}\left[G\left(\frac{\partial U}{\partial y}+\frac{\partial V}{\partial x}\right)\right]+\frac{\partial}{\partial z}\left[G\left(\frac{\partial U}{\partial z}+\frac{\partial W}{\partial x}\right)\right]=\rho\frac{\partial^2 U}{\partial t^2}$$

$$\frac{\partial}{\partial x}\left[G\left(\frac{\partial U}{\partial y}+\frac{\partial V}{\partial x}\right)\right]+\frac{\partial}{\partial y}\left[\lambda e+2G\frac{\partial V}{\partial y}\right]+\frac{\partial}{\partial z}\left[G\left(\frac{\partial V}{\partial z}+\frac{\partial W}{\partial y}\right)\right]=\rho\frac{\partial^2 V}{\partial t^2}$$

$$\frac{\partial}{\partial x}\left[G\left(\frac{\partial U}{\partial z}+\frac{\partial W}{\partial x}\right)\right]+\frac{\partial}{\partial y}\left[G\left(\frac{\partial V}{\partial z}+\frac{\partial W}{\partial y}\right)\right]+\frac{\partial}{\partial z}\left[\lambda e+2G\frac{\partial W}{\partial x}\right]=\rho\frac{\partial^2 W}{\partial t^2}$$

..... 3

where the volume expansion, or dilatation,

$$e = \frac{\partial U}{\partial x}+\frac{\partial V}{\partial y}+\frac{\partial W}{\partial z}\,,$$

and Lame's constant

$$\lambda = \frac{\nu E}{(1+\nu)(1-2\nu)} = \frac{2\nu G}{(1-2\nu)}$$

The equations of motion, given by equation (3), along with the appropriate boundary conditions describe the behavior of an isotropic dam in terms of displacement. Once the displacements are known, stresses are then determined by Hooke's law. In the general case of a non-homogeneous dam experiencing foundation motion due to an earthquake, E and G vary with position within the dam, and at any point they may also vary with the level of stress and the number of stress reversals. Due to the complicated nature of equation (3) and due to the irregular boundaries of a dam, the possibility of expressing the behavior in closed form is indeed very remote. In order to arrive at a feasible problem, many factors which complicate the behavior of a vibrating dam are assumed to have only a small effect on the total behavior and are therefore ignored. Numerical methods tend to have an advantage over exact methods for calculating behavior which includes the effects of the finer details of an actual dam.

A numerical method for solving the general equations of motion might proceed as follows. The differential equations of motion are replaced by a set of finite difference equations; that is, the parameters of equations (1) and (2) are approximated by a set of values defined at discrete points in the

material. At some time t, the deflected shape of the dam and the soil characteristics are known, and the distribution of stresses is obtained from Hooke's law. The three components of acceleration are then calculated from equation (1). These accelerations, acting for a small time step Δt, result in the incremental displacements ΔU, ΔV, and ΔW which are calculated by any of the various numerical integration techniques. The deflected shape of the dam is then calculated at time $t + \Delta t$ by superimposing ΔU, ΔV, and ΔW on the deflected shape associated with time t. This stepping procedure is then repeated many hundreds or even many thousands of times to obtain the dynamic behavior of an earth dam.

The advantages in a method of this type lie in its ability to calculate response at high levels of stress, even for stresses approaching failure. The modulus of elasticity, the modulus of rigidity, and the mass density can vary with position, stress, and time, although the density will probably vary only according to position in the structure. To obtain a good approximation of the dam, the zone size (the distance between the discrete points at which the parameters are defined) must be quite small, but for reasons of stability, the time step Δt must be less than the zone size divided by the speed of a traveling wave in the media[1]*. This restric-

---

*The superscripted numbers in brackets refer to references on page .

tion on the time interval may limit the use of this method for calculating response due to a long-duration earthquake to the extent that more approximate methods will be preferred.

Also, the method does not provide as much physical insight into the problem as would be desirable. It appears that this solution would offer little assistance in answering relevant questions such as: How is the compliance or stiffness of the foundation related to the internal stresses in the dam? How would a small change in geometry or soil characteristics of the dam affect the internal stresses? Methods which analyse the dynamic behavior of earth dams in terms of natural frequencies and mode shapes appear to offer more insight as to the effect of each parameter on the total behavior.

As might be expected, a general numerical solution for the nonlinear behavior of a three-dimensional dam poses an enormous computing problem, even for the largest digital computers. Methods which are less involved and therefore more feasible result from simplifying the characteristics of the dam. Often these simplifying assumptions are based on little more than intuition or engineering judgment. Some assumptions that are commonly made to simplify the analysis are as follows: (1) Vibrations in one or (more commonly) two directions can be ignored. (2) The response can be

considered to be linear; that is, strain is linearly dependent on stress. (3) Energy dissipation can either be ignored or can be treated by viscous modal damping.* (4) The dam can be analyzed as a homogeneous fill having an extremely simple geometry.

Mathematical Model of an Earth Dam

An approximate solution for the dynamic response of an earthfill dam is obtained by analyzing a simplified mathematical model. The characteristics of an earth dam that are considered to be predominately important dictate the model to be used.

An earth dam is a thick, massive structure with side slopes seldom steeper than 2:1, somewhat similar to a tapered cantilever beam oriented in the vertical direction. Vibration studies of short thick cantilever beams indicate that bending deflections are small in comparison to shear deflections (2). This suggests that the analysis of an earth dam might be simplified by ignoring bending deflections. Motohiro Hatanaka (3) has presented an approximate method for determining the effect of bending on the first natural frequency of an elastic wedge representing an infinitely long dam with a straight crest. Hatanaka concludes that ignoring the effects

---

*Viscous modal damping is explained later in Chapter III.

of bending for an earth dam with a Poisson's ratio of 0.35 and side slopes of 2:1 will result in a fundamental frequency which is too large by less than 10%, and for a dam with side slopes of 3:1, the natural frequency will be in error by only about 2.2%. Technically, these results do not fully indicate the effect of bending on the dynamic behavior of an actual dam because the motion of an actual dam is restrained by the abutments. Actually the effect that bending deflections have on the natural frequencies of the restrained dam are expected to be even less than for the infinitely long dam. At any rate, bending deflections are expected to play a minor role in the behavior of an earth dam and are therefore ignored in this analysis.

The geometry of the dam is approximated in the model by a homogeneous truncated wedge with end and bottom boundaries that can be fashioned to simulate the canyon walls.

The three-dimensional dam is then reduced to a two-dimensional mathematical model by assuming that the relative motions of points through the thickness of the dam in the upstream-downstrean direction are small, and therefore these relative motions are ignored. Also vertical and longitudinal vibrations are ignored. Thus, points in the idealized model used in this study have only one degree of freedom: transverse motion of the entire cross-section (rigid through the thickness). During an earthquake the amplitude of this

transverse motion will probably overshadow all other amplitudes of motion. Nevertheless, small vertical vibrations and small transverse vibrations through the thickness of the dam might play an important role in the failure of the dam. A more sophisticated application of the analytical technique used in this report which can include vibrations in the plane of a two-dimensional model is discussed later in the chapter titled "Recommendations for Future Work".

The analysis is further restricted by considering only linear response. To attempt to compute response at high levels of stress, the nonlinear characteristics of the soil would need to be included in the analysis, resulting in a much more complex problem. Although the simplified linear approach cannot be used when the dam is near failure, it is valuable in predicting when and where non-linearities first occur and possibly in estimating the extent of non-linear behavior.

This model is, admittedly, a crude representation of an earth dam. However, it will be shown that the model is adequate for predicting some of the major features of the vibrational behavior of an actual dam.

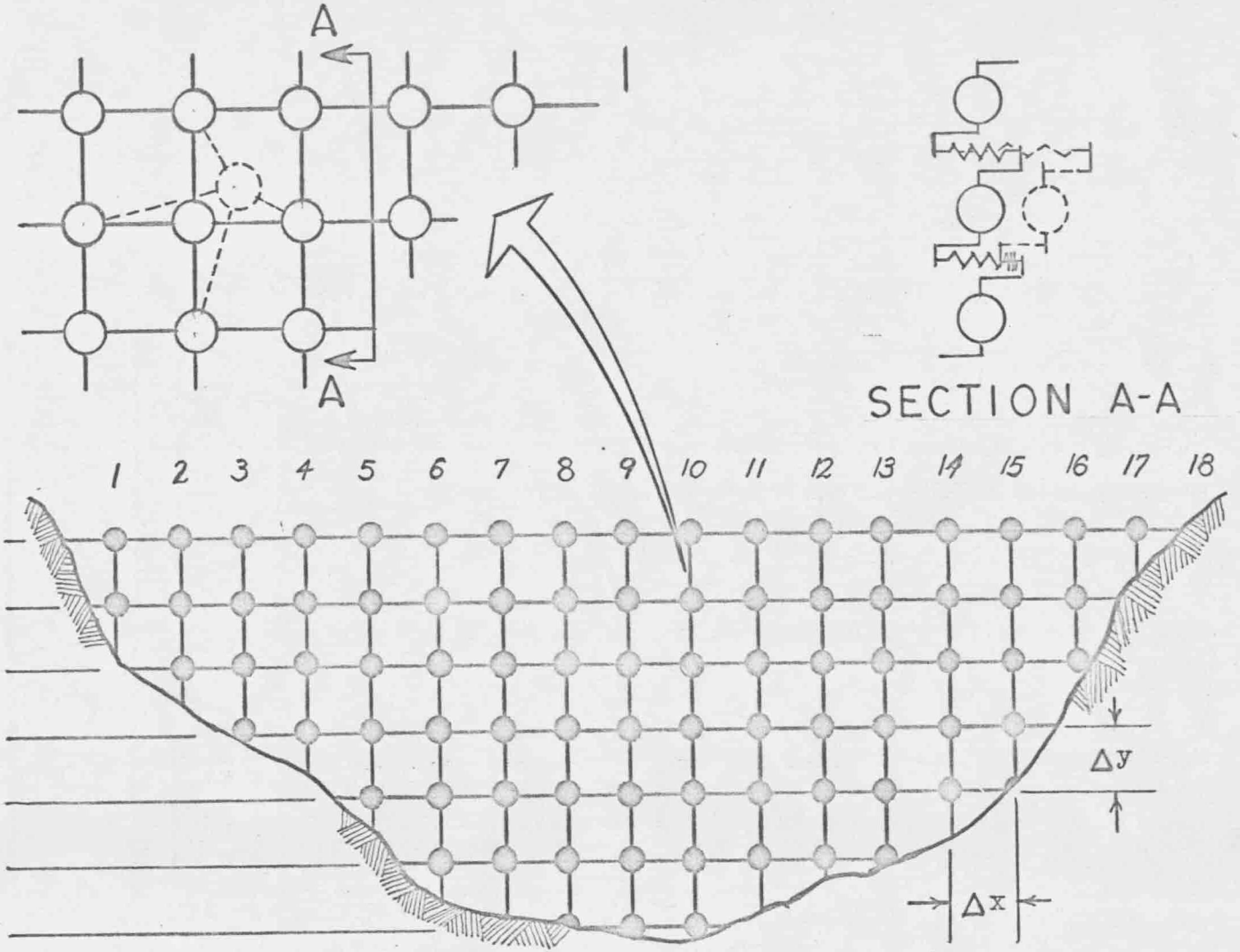
Chapter III

CALCULATING DYNAMIC BEHAVIOR

Calculating Natural Frequencies and Mode Shapes

The next step in the solution is the determination of natural frequencies and modes of vibrations of the model. It is reasonable to expect further alterations of the model when a method of solution is decided upon. For example, if an exact solution for the vibrations of the model is attempted, the irregular boundaries will necessarily have to be extremely simple. The most applicable exact solution presently available analyzes a model with rigid vertical ends and a rigid flat bottom. This solution, by Ambraseys (4), is used as a check on resonant frequencies obtained by the numerical method used in this paper.

In order to allow for arbitrary boundaries, the model is analysed as a rectangular grid of masses interconnected by shear resistant springs as illustrated in Figure 2. The mass-spring grid is the result of considering the dam to be composed of a finite number of rectangular blocks of earth, shown in Figure 3. Each point mass represents the mass of one block, and each spring stiffness represents the shear stiffness of the earth between the point masses. For ease of computations, all horizontal spacings between point masses are the same and all vertical spacings between point masses are the same.



Elevation View

Figure 2: Discrete Approximation of a Shear Dam

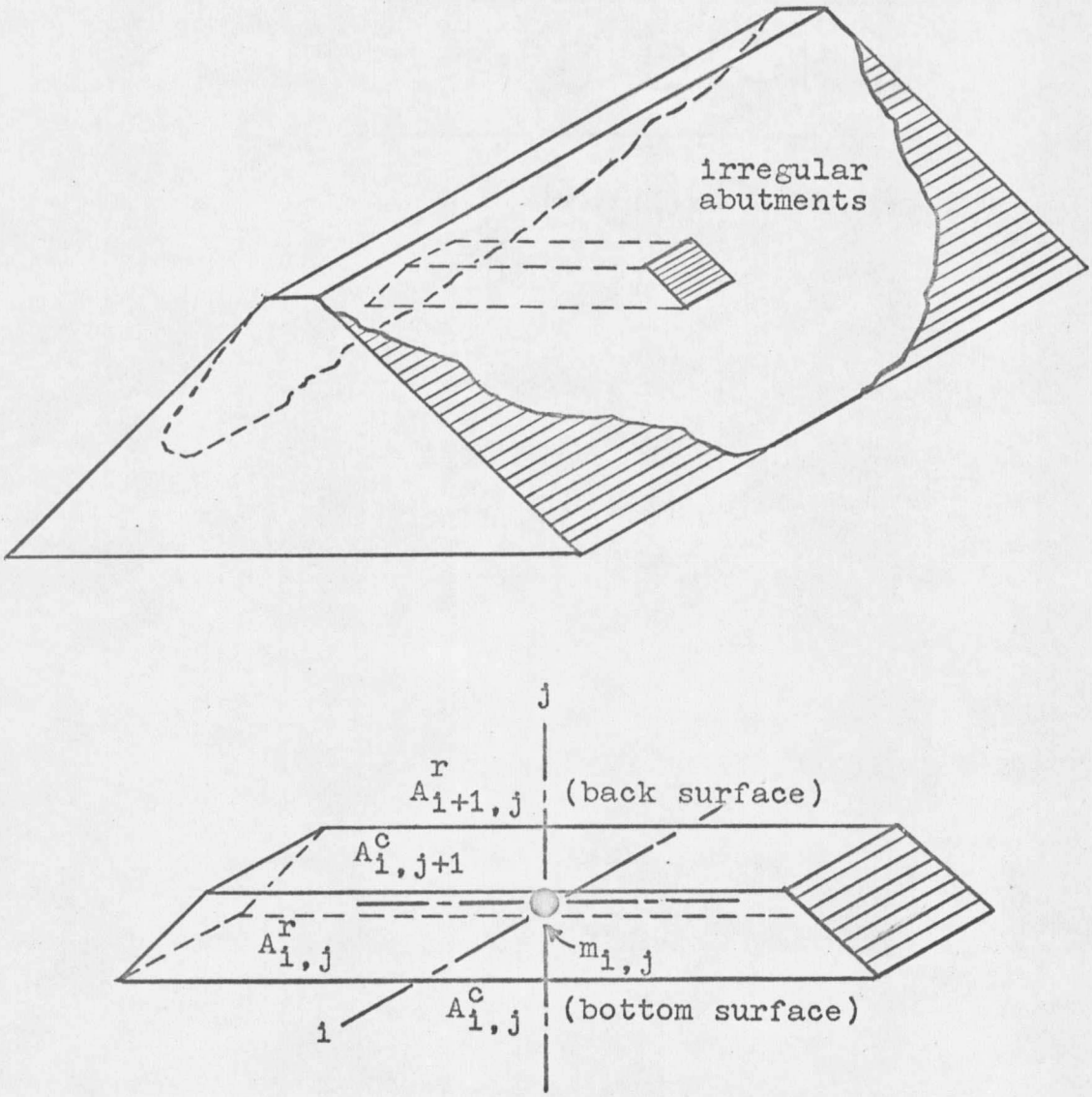


Figure 3: Block of Earth Represented by a Point Mass.

The most common method for calculating the natural frequencies and the mode shapes for such a mass-spring system is probably a matrix technique: The mass and spring characteristics of the dam are expressed in matrix form, [M] and [K], and the following eigenvalue problem is solved:

$$[M^{-1} K] U = \lambda U .$$

The natural frequencies are the square roots of the eigenvalues, λ_n, and the eigenfunctions, U_n, give the mode shapes. Although this method is available, an extension of Holzer's Method is used here in order to investigate the advantages that the method might have for two-dimensional problems.

Holzer's Method was originally presented for a one-dimensional system of masses connected in a chain-like fashion by torsion springs [5]. Later Prohl and Myklestad extended the method to one-dimensional flexural members [6,7]. Keightley then went one step further and applied the method to a two-dimensional framework, vibrating in the plane of the framework [8]. Thus, all previous work with the Holzer Method has been restricted to systems with chain-like topology.

In Holzer's scheme a system is assumed to be vibrating sinusoidally at some angular frequency ω_1, with all points moving in phase. If this assumed frequency is a natural frequency of the system, no external excitation is required

for sustained motion. That is to say, the internal restoring forces in the structure are of exactly the right magnitude to cause the accelerations of all of the masses. Generally, however, the assumed frequency is not a natural frequency, in which case steady-state external excitation is required at some point to keep the system vibrating at the assumed frequency. If a different frequency of vibration is assumed, say ω_2, it will be found that a different steady-state excitation is required, thus establishing a trend for determining a frequency ω_3 which requires less excitation than either ω_1 or ω_2. After refining the frequency a sufficient number of times, a frequency ω_n is obtained at which only a negligible steady-state excitation is required to keep the system vibrating. Thus a natural frequency is located.

In the solution of the two-dimensional mass-spring system of Figure 2, all points are assumed to be vibrating in phase at a constant angular frequency ω. The transverse deflection $U_{i,j}(t)$ of the mass point $m_{i,j}$ of Figure 2 is expressed by:

$$U_{i,j} = \overline{U}_{i,j} \operatorname{Sin} \omega t$$

where $\overline{U}_{i,j}$ is the amplitude of transverse deflection of $m_{i,j}$. The first subscript stands for the row location and the second subscript for the column location of an element.

The transverse acceleration $a_{i,j}(t)$ can then be expressed as follows:

$$a_{i,j} = \ddot{U}_{i,j} = - \omega^2 \bar{U}_{i,j} \text{ Sin } \omega t = - \omega^2 U_{i,j}$$

where $\ddot{U}_{i,j}$ signifies the second derivative of $U_{i,j}$ with respect to time. The sum of the external forces on $m_{i,j}$ can then be expressed:

$$\Sigma \text{ forces on element } (i,j) = m_{i,j}\, a_{i,j} = -m_{i,j}\, \omega^2 U_{i,j}.$$

Acting on each concentrated mass are the transverse shear forces applied by the four shear springs associated with each concentrated mass. A shear spring represents the shear resistance of the soil contained between two mass points. By applying Hooke's law and adopting the sign convention that the deflection $U_{i,j}$ into the paper is positive, and a shear force acting out of the paper on the mass point $m_{i,j}$ of Figure 2 is positive when located to the left of or below the mass, and negative when located to the right of or above the mass, the following equations can be written:

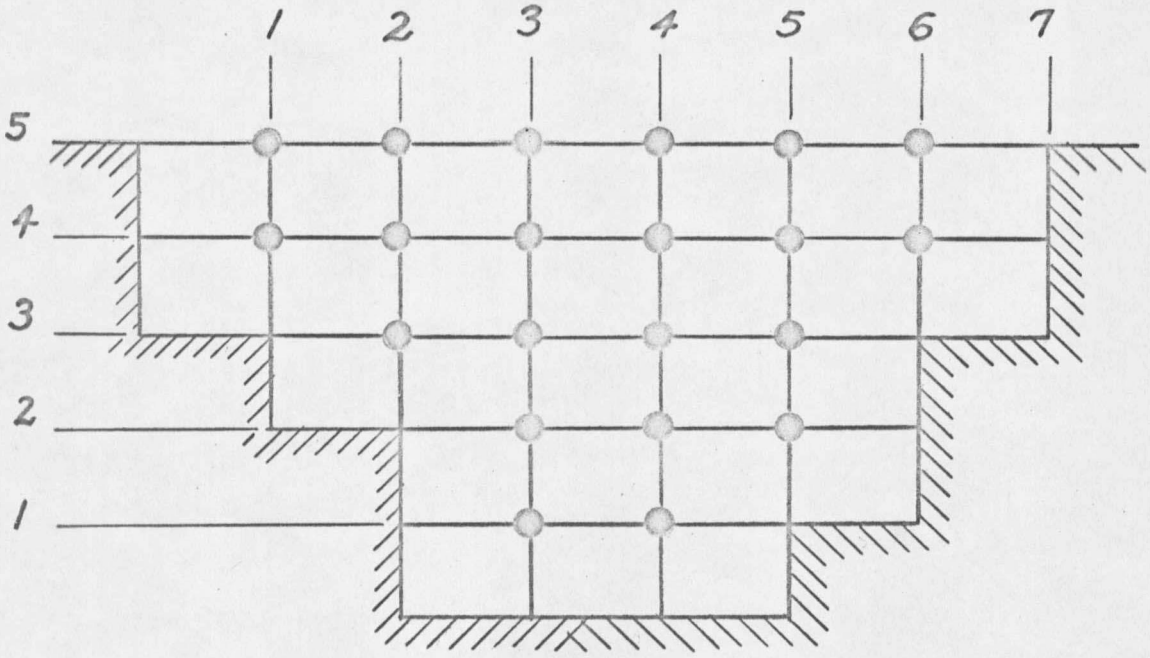
$$U_{i,j} = U_{i,j-1} + \frac{V^r_{i,j} \Delta x}{A^r_{i,j}\, G} \qquad \text{.....} \qquad 4$$

$$V^c_{i,j} = (U_{i,j} - U_{i-1,j}) \frac{G\, A^c_{i,j}}{\Delta y} \qquad \text{.....} \qquad 5$$

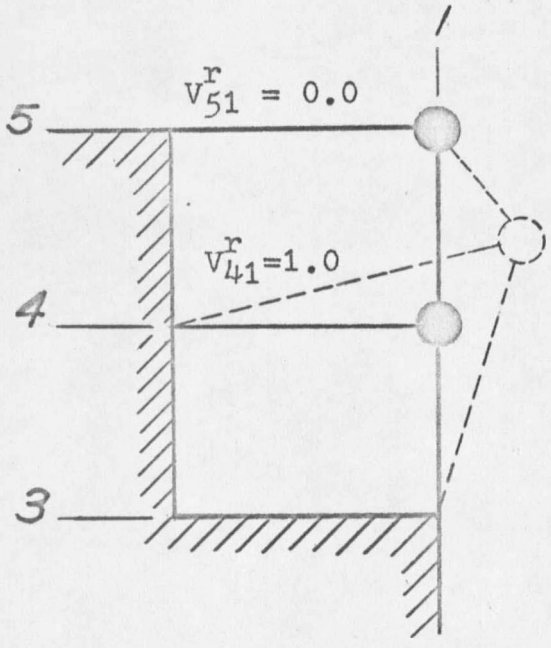
$$V^r_{i,j+1} = V^r_{i,j} + V^c_{i,j} - V^c_{i+1,j} - \omega^2 m_{i,j} U_{i,j} \quad \cdots\cdots \quad 6$$

where $V^r_{i,j}$ is the transverse shear in the horizontal spring between $m_{i,j}$ and $m_{i,j-1}$, $V^c_{i,j}$ is the transverse shear in the vertical spring between $m_{i,j}$ and $m_{i-1,j}$. $A^r_{i,j}$ is the area of the vertical surface common to the element of soil at (i,j) and the element of soil at (i,j-1), and $A^c_{i,j}$ is the area of the horizontal surface common to the element of soil at (i,j) and the element of soil at (i-1,j). G is the modulus of rigidity, and Δx and Δy are respectively the horizontal and vertical distances between mass points.

Successive application of equations (4), (5) and (6) lead to a step-by-step calculation of all the shears and the deflections of the mass-spring grid, provided a sufficient number of shears and deflections are known initially. If the mass-spring system of Figure 4(a) is vibrating at the frequency ω_1 and the shear force in each horizontal spring connecting to the left abutment is zero except the shear in the fourth spring which is unity, then the deflection of each mass point in column 1 is determined by equation (4), and the shear in each vertical spring of column 1 is determined by equation (5) as shown in Figure 4(b). The shear in each of the horizontal springs connecting column 1 to column 2 is determined by equation (6). The deflection of every mass point and the shear in every spring associated with column



(a)



$$U_{51} = 0.0 \quad \ldots\ldots\ldots\ldots \quad \text{eq.(4)}$$

$$V^c_{51} = (U_{51} - U_{41}) \frac{GA^c_{51}}{\Delta y} \quad \ldots \quad \text{eq.(5)}$$

$$U_{41} = V^r_{41} \frac{\Delta x}{A^r_{41} G} \quad \ldots\ldots\ldots \quad \text{eq.(4)}$$

$$V^c_{41} = (U_{41} - U_{31}) \frac{GA^c_{41}}{\Delta y} \quad \ldots \quad \text{eq.(5)}$$

$$U_{31} = 0.0 \quad \ldots\ldots\ldots\ldots \quad \text{assigned}$$

(b)

Figure 4: Mass-Spring Grid Illustrating the Step-by-Step Procedure for Calculating Internal Shears and Deflections.

2 is then calculated by the application of equations (4), (5) and (6) in a similar manner. Proceeding from left to right, the deflection of every mass point and the shear in every spring in the model are determined by the successive application of equations (4), (5) and (6).

In general the deflections computed at the extreme right side of the net will not be zero, but for the trial frequency ω_1, the deflections are linearly dependent on $V^r_{4,1}$. That is

$$U_{1,5} = C_{1,4}\, V^r_{4,1}$$

$$U_{2,6} = C_{2,4}\, V^r_{4,1}$$

$$U_{3,6} = C_{3,4}\, V^r_{4,1}$$

$$U_{4,7} = C_{4,4}\, V^r_{4,1}$$

$$U_{5,7} = C_{5,4}\, V^r_{4,1} \cdots$$

where the constants $C_{i,4}$ are the deflections at the extreme right side of the net due to the unit shear force $V^r_{4,1}$ on the left side of the net.

Now if $V^r_{4,1}$ is set to zero and $V^r_{5,1}$ is assigned a shear force of unity, and the same frequency ω_1 is assumed, the linear relationship between the right boundary deflections and $V^r_{5,1}$ can be determined by successive application of equations (4), (5) and (6) as outlined for $V^r_{4,1}$. Similarly

the linear relationships between all of the left boundary shears and the right boundary deflections are determined and the following equations result:

$$\begin{Bmatrix} U_{1,5} \\ U_{2,6} \\ U_{3,6} \\ U_{4,7} \\ U_{5,7} \end{Bmatrix} = \begin{bmatrix} C_{1,1} & C_{1,2} & C_{1,3} & C_{1,4} & C_{1,5} \\ C_{2,1} & C_{2,2} & C_{2,3} & C_{2,4} & C_{2,5} \\ C_{3,1} & C_{3,2} & C_{3,3} & C_{3,4} & C_{3,5} \\ C_{4,1} & C_{4,2} & C_{4,3} & C_{4,4} & C_{4,5} \\ C_{5,1} & C_{5,2} & C_{5,3} & C_{5,4} & C_{5,5} \end{bmatrix} \begin{Bmatrix} V^r_{1,3} \\ V^r_{2,3} \\ V^r_{3,2} \\ V^r_{4,1} \\ V^r_{5,1} \end{Bmatrix} \quad \cdots \quad 7$$

As discussed earlier, the magnitude of external excitation is used as a guide for locating natural frequencies. The only possibility for external excitation is through the movement of the points on the extreme right of the net since no external driving force has been included in the procedure up to this point. If ω_1 is a natural frequency, no external excitation is required to keep the system vibrating, and the displacement of the right abutment, $\{U\}$ of equation (7), must be zero. Ignoring the trivial case of $\{V\} = 0$, this condition requires that the determinant of $[C]$ must be zero. In general, for arbitrary choice of ω_1, the determinant of $[C]$ is not zero, but it can be used as a guide for locating natural frequencies. Thus if a different frequency ω_2 is assumed, and

a new set of coefficients is obtained whose determinant is different from the determinant associated with ω_i, a trend is established for locating a frequency for which the determinant of coefficients will be very small. The frequency that results in a set of coefficients with a zero determinant is a natural frequency of the structure. That is to say the system will have sustained free vibration.

The mode shape at the natural frequency ω_n is determined by solving the linear homogeneous matrix equation (7) for the left boundary shears by assigning one of the shears, say $V^r_{5,1}$, a value of unity, thus normalizing the solution. These left boundary shear values then lead to a step-by-step determination of all the shears and deflections of the grid of Figure 4. Often it is desirable to normalize the mode shape so that the maximum displacement is unity. This can be accomplished by dividing all shears and deflections by the maximum deflection of the grid.

General Response Due To Arbitrary Boundary Motion

The knowledge of the natural frequencies and their corresponding mode shapes is used to determine the linear response of an earth dam subjected to an arbitrary boundary disturbance. The amplitude of response is a linear function of the amplitude of the boundary motion and is dependent on the frequency spectrum of the boundary motion in a more

complicated manner. The frequency components of the boundary motion which are near the natural frequencies of the dam cause a larger amplification of response than frequency components which are well away from any natural frequencies of the dam.

A dam is generally quite a long structure; a length in excess of 1000 feet is not uncommon. In general, points along the boundary of a dam which is experiencing a seismic disturbance do not have the same transverse motion at the same instant of time. The importance of including the non-rigid boundary motion in the analysis is emphasized by the following considerations: A shear wave which is traveling at 2,000 feet per second in the foundation rock adjacent to a dam is considered. If the shear wave is traveling in a direction which makes an angle θ with the crest of the dam, the ground motion, which is perpendicular to the direction of wave propagation, makes an angle of $90^{\circ} - \theta$ with the crest, shown in Figure 5(a). The component of the seismic shear wave which excites the dam at its fundamental frequency, assumed to be 5.0 cps, is considered. It should be noted that ground motion at a frequency of 5.0 cps is very common and therefore is of particular interest. This seismic wave, having a frequency of 5.0 cps and traveling at 2,000 feet per second, has a wave length L = 400 feet. The effective wave length along

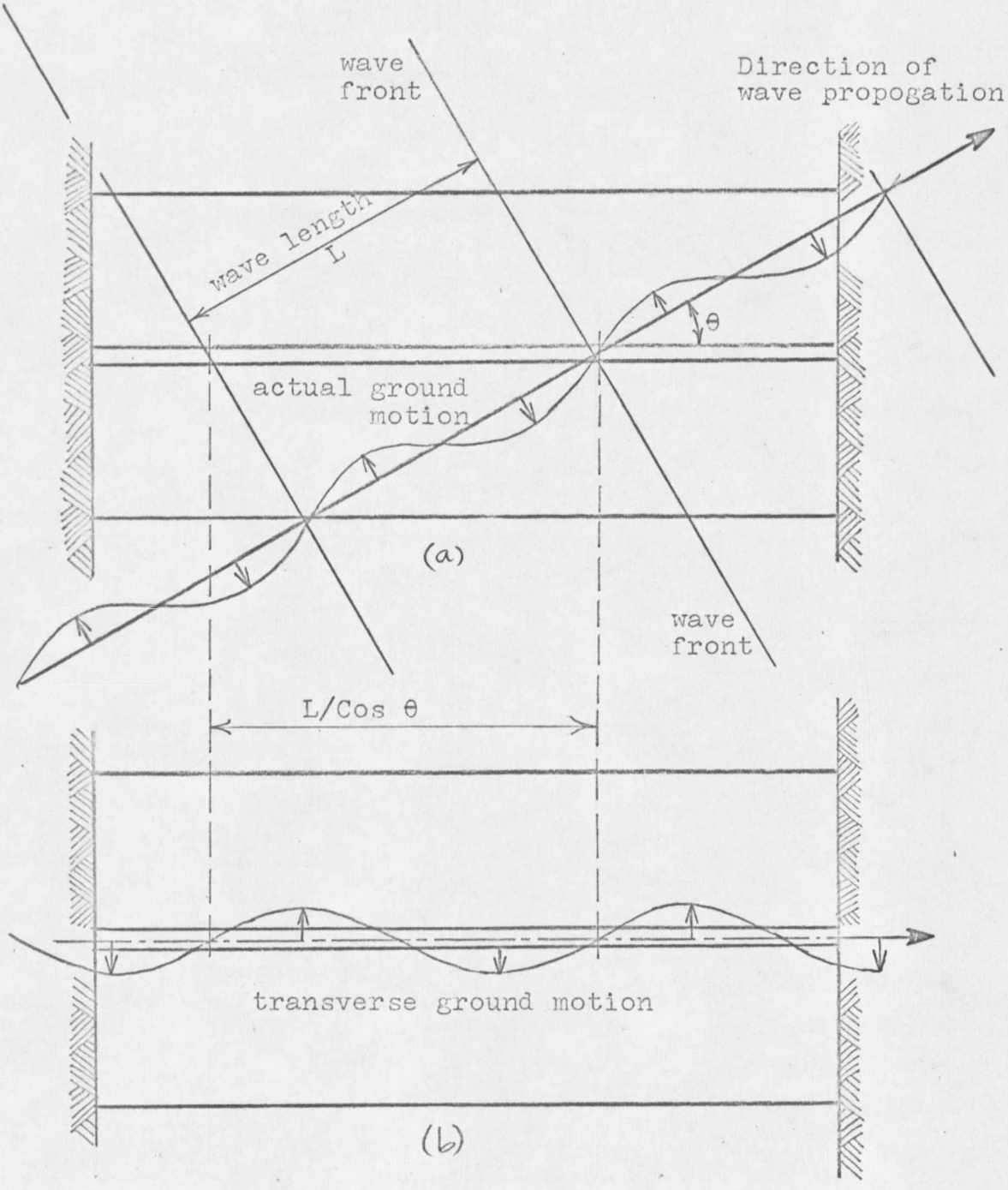


Figure 5: Plan View of an Earth Dam Showing Seismic Waves Approaching at an Oblique Angle.

the crest of the dam is $L/\cos\theta$, shown in Figure 5(b). The typical seismic wave shown in Figure 5 clearly illustrates the need for a method which can include the effects of non-rigid boundary motion.

The response of the dam to non-rigid boundary motion is obtained by superimposing the response due to the motion of each boundary point separately. That is, each boundary point is to experience some arbitrary motion, and the displacement response of the entire dam resulting from the motion of only one boundary point at a time is calculated. These partial solutions are then added together in the proper manner to achieve the effect of a traveling wave moving across the dam. If a wave is moving from left to right across the dam, as shown in Figure 5, the boundary point (or points) on the extreme left of the dam experiences the motion of the wave slightly before the other boundary points on the dam. The boundary point (or points) in column 1 of the net, shown in Figure 4, experiences the same motion as the extreme left of the dam, except that the motion of column 1 lags by a small time step which depends on: the velocity of the propagating wave in the underlying foundation rock, the approach angle of the traveling wave relative to the longitudinal axis of the dam, and the horizontal grid size of the net, shown in Figure 4.

The displacement response of the dam due to the motion of a particular boundary point can be considered to be composed of a static component and a dynamic component, U_s and U_d. Both U_s and U_d are functions of the horizontal and vertical coordinate location on the dam, and the dynamic component is also a function of time. The static component serves to satisfy the boundary conditions of the vibrating dam but contributes nothing toward satisfying the differential equation which governs the motion of the interior of the vibrating dam. The dynamic component, on the other hand, satisfies the differential equation of motion for the interior of the vibrating dam, and contributes nothing to the boundaries of the dam. Thus the total solution which is composed of a static component and a dynamic component is truly a solution to the differential equation of motion for the interior of the dam and satisfies the boundary conditions of the dam.

The statically deflected shape of the dam resulting from a unit deflection of the particular boundary point (i,j) is designated as $U_s(i,j)$. The two-dimensional Holzer Method is used to solve this static problem. All of the bottom boundary points and the left boundary points, with the exception of point (i,j), are assigned a zero deflection, and the right boundary is considered to be detached from the right abutment. At zero frequency the deflections at the extreme right of the

grid are expressed in terms of left boundary shears as described by equation (7) of the previous section.

If the boundary point (i,j) which is assigned a unit deflection is on the right boundary, all of the right boundary points appearing in equation (7) are assigned a zero deflection except the boundary point (i,j) which is assigned a unit deflection. The left boundary shears corresponding to this deflected shape are calculated directly from equation (7), and the statically deflected interior $U_s(i,j)$ is calculated, working from left to right, by the step-by-step procedure previously described.

The procedure for calculating $U_s(i,j)$ is slightly different when the boundary point (i,j) is not on the right boundary. All of the left boundary springs are assigned a zero shear and the boundary point (i,j) is assigned a unit deflection. The deflections at the right of the grid due to the unit deflection of the boundary point (i,j) are then calculated by proceeding from the deflected point (i,j) to the right, using equations (4), (5) and (6) as described earlier. Now the deflections on the right boundary shears are calculated from equation (7) to exactly cancel the right boundary deflections due to the unit deflection of the boundary point (i,j). Starting with these left boundary shears and working to the right across the grid, the statically

deflected interior $U_s(i,j)$ is calculated.

The dynamic displacement response $U_d(i,j,t)$ due to the motion of the particular boundary point (i,j) must satisfy the differential equation of motion for the dam with homogeneous boundary conditions (zero boundary deflections). The general solution to an inhomogeneous differential equation can always be expressed as a formal sum over the eigenfunctions of the homogeneous equation by use of a Green's function. This fact allows U_d to be expressed as a linear combination of the normal modes Φ_m as follows:

$$U_d(i,j,t) = \sum_m c_m(t)\ \Phi_m \qquad \ldots\ldots\ldots\ldots \quad 8$$

where $c_m(t)$ is the participation factor of the m^{th} normal mode Φ_m at time t. The modes Φ_m are arranged according to frequency with Φ_1 representing the fundamental mode shape.

The total displacement $U_t(i,j,t)$ of the interior of the dam due to the motion of the boundary point (i,j), expressed as the static component plus the dynamic component, is::

$$U_t(i,j,t) = B(i,j,t)\ U_s(i,j) + U_d(i,j,t)$$

where $B(i,j,t)$ represents the transverse displacement of boundary point (i,j) expressed as a function of time. In shorter notation:

$$U_t = B\ U_s + \sum_m c_m\ \Phi_m\,, \qquad \ldots\ldots\ldots\ldots \quad 9$$

and total acceleration $\ddot{U}_t$ of the interior of the dam is:

$$\ddot{U}_t = \ddot{B}\, U_s + \sum_m \ddot{c}_m \Phi_m \qquad \text{..... 10}$$

where $\ddot{U}_t$ is the second derivative of U_t with respect to time.

The general form for the equation of motion for the elastic dam is:

$$L(U_t) = \rho \ddot{U}_t \qquad \text{..... 11}$$

where $L(U_t)$ is the elastic restoring force per unit volume and ρ is the mass density. The linear operator L for a dam which has a linear taper from the base to the crest is derived in Appendix A and has the form:

$$L(U_t) = G\left[\frac{\partial^2 U}{\partial x^2} + \frac{\partial^2 U}{\partial y^2} + \frac{1}{y}\frac{\partial U}{\partial y}\right].$$

Linearity of the operator L allows the restoring force to be separated into a restoring force due to the dynamic component of deflection and a restoring force due to the static component of deflection as follows:

$$L(U_t) = L(U_d) + L(U_s)$$

But the restoring force $L(U_s) = 0$ since the dam is not accelerating as the result of U_s, thus:

$$L(U_t) = L(U_d)$$

or making use of equation (8)

$$L(U_t) = L\left(\sum_m c_m \Phi_m\right) .$$

or

$$L(U_t) = \sum_m c_m L(\Phi_m) .$$

But, the mode shape, Φ_m, is defined by the relationship:

$$L(\Phi_m) = - \omega_m^2 \Phi_m ;$$

therefore, the elastic restoring force assumes the form:

$$L(U_t) = \sum_m c_m(- \omega_m^2 \Phi_m) .$$

Substituting this form for $L(U_t)$ into equation (11) along with $\ddot{U}_t$ of equation (10) gives:

$$\sum_m c_m(-\rho \omega_m^2 \Phi_m) = \rho(\ddot{B} U_s + \sum_m \ddot{c}_m \Phi_m) .$$

or

$$\sum_m (\ddot{c}_m + \omega_m^2 c_m) \Phi_m = -\ddot{B} U_s .$$

Multiplying both sides by $\Phi_n \, dV$ and integrating over the volume, V, gives:

$$\sum_m (\ddot{c}_m + \omega_m^2 c_m) \int_V \Phi_m \Phi_n \rho dV = -\ddot{B} \int_V \Phi_n U_s \rho dV \quad ..... \; 12$$

Orthogonanity of the modes requires $\int_V \Phi_m \Phi_n \, dV = 0$ for $m \neq n$ (derivation given in Appendix B); therefore, equation (12) becomes:

$$(\ddot{c}_n + \omega_n^2 c_n) \int_V \Phi_n^2 \rho dV = -\ddot{B} \int_V \Phi_n U_s \rho dV$$

or

$$\ddot{c}_n + \omega_n^2 c_n = Q_n(t) \quad \ldots\ldots\ldots\ldots \quad 13$$

where

$$Q_n(t) = -B \frac{\int_V \Phi_n U_s \rho \, dV.}{\int_V \Phi_n^2 M_{el} \rho \, dV}$$

A more appropriate form for $Q_n(t)$ is

$$Q_n(t) = -\ddot{B} \frac{\sum_{el} \Phi_n U_s M_{el}}{\sum_{el} \Phi_n^2 M_{el}} \quad \ldots\ldots\ldots \quad 14$$

where $\rho \, dV$ is replaced by the mass of an element M_{el} of Figure 3 and the integral over the volume is replaced by the summation over all the elements.

The participation factor c_n of the n^{th} normal mode due to the motion experienced by the particular boundary point (i,j) can be calculated from equation (13), since the equivalent forcing function $Q_n(t)$ is expressed in terms of known quantities by equation (14). It should be noticed that equation (13) is the equation of motion for the simple mass-spring system of Figure 6 with the viscous damping C omitted. Thus the contribution of the normal mode Φ_n is equivalent to the displacement response of a simple mass-spring system with

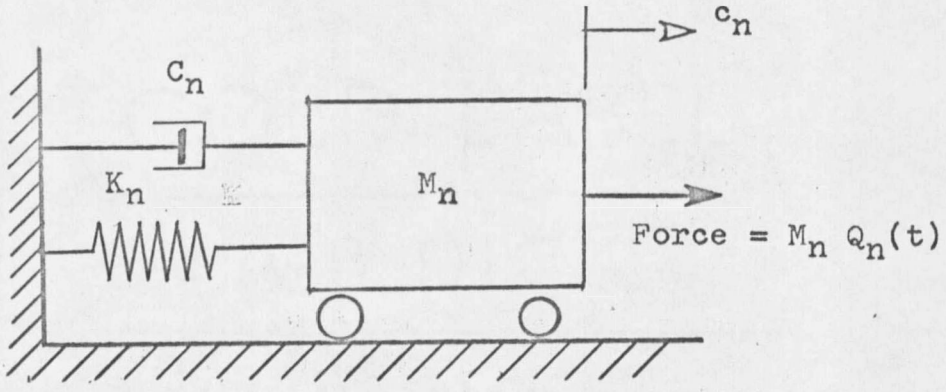


Figure 6: Single Degree of Freedom System.

the same natural frequency ω_n that is associated with Φ_n. The forcing function $Q_n(t)$ applied to the simple mass-spring system differs from the acceleration $\ddot{B}$ of the boundary point (i,j) by a constant which indicates the sensitivity of the mode Φ_n to accelerations of the boundary point (i,j).

In an actual structure the free vibrations resulting from a boundary disturbance will die out soon after the disturbance stops. Equation (13) has no factor to dampen the solutions; therefore, the calculated vibrations will not diminish with time. This may result in a gross misrepresentation of the contribution of each mode a few seconds after the boundary disturbance begins. To control this cumulative error, modal damping is introduced, illustrated by the viscous damping coefficient C appearing in Figure 6. Modal damping is the result of considering the dam to have only viscous damping which is acting in such a manner that all damped modes have the same shape as the undamped modes. Experimental results taken from Bouquet Dam (8) show some indication that this hypothetical concept of energy dissipation can give suitable results at low levels of stress. Calculated (undamped) mode shapes are compared with measured mode shapes later in the section titled Dynamic Behavior of Bouquet Dam.

The revised equation for the participation factor c_n then becomes:

$$\ddot{c}_n + \frac{C}{M}\dot{c}_n + \omega_n^2 c_n = Q(t) \quad \ldots\ldots\ldots \quad 15$$

where M is the mass of the simple mass-spring system of Figure 6. The magnitude of C and M have no direct relationship to the physical dam, but their ratio becomes meaningful when written in the form, $\frac{C}{M} = 2\zeta\omega_n$, since ζ, the ratio of C to critical damping, can be measured experimentally. Equation (15) then becomes:

$$\ddot{c}_n + 2\zeta\omega_n \dot{c}_n + \omega_n^2 c_n = Q(t) . \qquad \text{.....} \quad 16$$

It is emphasized that the damping is added to cause the free vibrations to diminish with time, but the natural frequencies and their corresponding mode shapes are calculated from an undamped system.

Arbitrary boundary motion will complicate the method for solving equation (16) since Q(t) will also be arbitrary. An analog computer might be used to solve the equation very nicely. Considerable complications arise, however, in connecting this portion of the solution to the rest of the solution which is carried out by a digital computer. To escape the complications of the hybrid computer system, the general solution of equation (16) is found by numerically integrating Duhamel's integral:

$$c_n(t) = \int_0^t Q_n(t') H_n(t-t') \, dt' \qquad \text{.....} \quad 17$$

$H_n(t-t')$ is the Green's function of equation (16) which is

merely the response, c_n of Figure 6, resulting from a force impulse applied at time t' and is given by:

$$H_n(t-t') = \frac{e^{-\zeta\omega_n(t-t')}}{\omega_n\sqrt{1-\zeta^2}} \operatorname{Sin}\ \omega_n\sqrt{1-\zeta^2}(t-t') \quad \ldots. \quad 18$$

Substituting $H_n(t-t')$ from equation (18) into equation (17) and expanding gives:

$$c_n(t) = \frac{e^{-\zeta\omega_n t}}{\omega_{dn}}\left[\operatorname{Sin}\omega_{dn}t\int_o^t e^{\zeta\omega_n t'}\operatorname{Cos}\omega_{dn}t'\ Q(t')\,dt'\right.$$

$$\left.-\operatorname{Cos}\omega_{dn}t\int_o^t e^{\zeta\omega_n t'}\operatorname{Sin}\omega_{dn}t'\ Q(t')\,dt'\right] \quad 19$$

where the notation ω_{dn} represents the damped natural frequency $\omega_n\sqrt{1-\zeta^2}$. The expanded form of equation (19) allows the integration to proceed by steps, that is:

$$\int_o^{t_n} F(t,t')\,dt' = \int_o^{t_1} F(t,t')\,dt' + \int_{t_1}^{t_2} F(t,t')\,dt' + \cdots +$$

$$+ \int_{t_{n-1}}^{t_n} F(t,t')\,dt'$$

where the integrand $F(t,t')$ is any arbitrary function of t and t'. The calculations involved in obtaining the value c_n at various designated times along a seismic disturbance are simplified considerably by this cumulative integration

relationship. The value $c_n(t_1)$ is calculated from equation (19) by numerically performing the indicated integration from $t = 0$ to $t = t_1$. The value of the integrals thus obtained can be used again to shorten the calculations for obtaining $c_n(t_2)$ where $t_2 > t_1$.

The total displacement response due to the arbitrary motion of the particular boundary point (i,j) is now calculated by substituting c_n, from equation (19), into equation (9). The displacement response due to the motion of each of the other boundary points is determined in a similar manner, and the results are superimposed to give the total displacement response due to the entire boundary disturbance. Thus it is possible that each point along the boundary may be experiencing an arbitrary motion completely independent of the motion of the other boundary points. Of more practical value however, each point along the boundary may be experiencing the same motion, but the motion does not occur at the same time for each boundary point. The traveling-wave effect is achieved by assigning the motion of each boundary point with the proper time lag relative to the motion of some reference point, say the extreme left of the dam.

Chapter IV

CALCULATED BEHAVIOR

Computer Code

A FORTRAN II computer code has been developed to compute the linear response in the upstream-downstream direction of an idealized earth dam experiencing arbitrary horizontal boundary motion perpendicular to the longitudinal axis of the dam.

The computer code is divided into the following steps:

1. The dam is subdivided into a lumped-mass system as shown in Figure 2.
2. The natural frequencies and their associated mode shapes are calculated.
3. The displacement and the acceleration time histories of one point on the boundary are computed from a digitized time history of velocity which might represent the record of an earthquake or some other seismic disturbance. The displacement, velocity, and acceleration time histories of all the remaining boundary points are then calculated from the known (or assumed) velocity of the traveling seismic waves in the foundation rock adjacent to the dam and the known (or assumed) direction that the waves are traveling with respect to the dam.

4. The total displacement response, due to the boundary motion calculated in step 3, is calculated at any designated time. The average transverse internal shear stresses in the dam are then calculated from a linear stress strain relationship.

A check on the total code is accomplished by checking each step separately. Steps (1) and (3) are both checked by hand calculations, and step (2) is checked by a comparison with an exact solution, presented in the next section. A method for checking the calculation carried out in step (4) is presented in Appendix C.

Mathematical Check on Natural Frequencies and Mode Shapes

Both a check on step (2) of the code and a feeling for the effect of the grid size of the model are obtained by comparing calculated natural frequencies and mode shapes with the natural frequencies and mode shapes obtained from the exact solution to the differential equation of motion for a truncated shear wedge with rigid vertical ends and a rigid flat bottom, as presented by Ambraseys[4].

The differential equation which describes the transverse motion of the undamped shear wedge of Figure 7, given previously by equation (11) and derived in Appendix A, is:

$$G\left[\frac{\partial^2 U}{\partial x^2}+\frac{\partial^2 U}{\partial y^2}+\frac{1}{y}\frac{\partial U}{\partial y}\right]=\rho\frac{\partial^2 U}{\partial t^2} \qquad \text{.....} \quad 20$$

The boundary conditions associated with the wedge are:

$$U = 0 \text{ at } x = 0, L \qquad \text{.....} \quad 21$$

$$U = 0 \text{ at } y = H \qquad \text{.....} \quad 22$$

$$\sigma_{yz} = G\frac{\partial U}{\partial y} = 0 \text{ at } y = h' \qquad \text{.....} \quad 23$$

where L, H, and h' are shown in Figure 7. It should be noticed that the natural frequencies and mode shapes obtained from the solution of equation (20) should exactly agree with the natural frequencies and mode shapes calculated from a grid similar to the one pictured in Figure 2 for the limiting case of an infinitely fine grid.

The method of separation of variables is used to simplify equation (20), i.e. it is assumed that $U(x,y,t) = X(x)\,Y(y)\,T(t)$. Substituting this expression for U into equation (20) and separating the variables gives:

$$S^2\left[\frac{1}{X}\frac{d^2X}{dx^2}+\frac{1}{Y}\frac{d^2Y}{dy^2}+\frac{1}{y}\frac{1}{Y}\frac{dY}{dy}\right]=\frac{1}{T}\frac{d^2T}{dt^2} \qquad \text{.....} \quad 24$$

where the shear wave velocity of the material is given by $S = \sqrt{G/\rho}$. Since x, y, and t are independent, the terms of equation (24) are also independent; and therefore, each independent term must be a constant. This leads to:

$$\frac{1}{T}\frac{d\,T}{dt^2} = -\omega^2 , \qquad \text{.....} \qquad 25$$

$$\frac{1}{X}\frac{d^2X}{dx^2} = -k^2 , \qquad \text{.....} \qquad 26$$

and

$$\frac{1}{Y}\frac{d^2Y}{dy^2} + \frac{1}{y}\frac{dY}{dy} = k^2 - \frac{\omega^2}{S^2} \qquad \text{.....} \qquad 27$$

where ω^2 and k^2 are constants to be determined. Equation (25) gives:

$$T(t) = A \operatorname{Sin} (\omega t - \alpha).$$

Similarly equation (26) gives:

$$X(t) = C \operatorname{Sin} kx + D \operatorname{Cos} kx,$$

but equation (21) requires that $D = 0$ and $k = \frac{r\pi}{L}$ where r is an integer which specifies the longitudinal modes of vibration. Thus

$$X(x) = C \operatorname{Sin} \frac{r\pi}{L} x .$$

Equation (27) is recognized as a zero order Bessel equation with the general solution:

$$Y(y) = A' J_o(\beta y) + B' Y_o(\beta y)$$

where

$$\beta = \left[(\omega/S)^2 - \left(\frac{r\pi}{L}\right)^2 \right]^{\frac{1}{2}} .$$

Equation (22) is satisfied by assigning

$$A' = Y_o(\beta H)$$

and

$$B' = -J_o(\beta H) .$$

Equation (23) requires that

$$-Y_o(\beta H)\, J_1(\beta h') + J_o(\beta H)\, Y_1(\beta h') = 0 \quad \ldots\ldots\ldots \quad 28$$

This equation is satisfied only by discrete values of β, say β_n, where n is an integer which specifies the vertical mode of vibration.

The equation for the $(n,r)^{th}$ mode of vibration, which is of the form $U_{nr} = X_r(x)\, Y_n(y)\, T_{nr}(t)$, is then given by:

$$U_{nr} = Y_o(\beta_n H)\, J_o(\beta_n y) - J_o(\beta_n H)\, Y_o(\beta_n y) \cdot \operatorname{Sin}\left(\frac{r\pi x}{L}\right) \operatorname{Sin}(\omega_{nr} t - \alpha), \quad \ldots\ldots\ldots\ldots \quad 29$$

and the associated natural frequencies are given by:

$$\omega_{nr} = S\left[\beta_n^2 + \left(\frac{r\pi}{L}\right)^2\right]^{\frac{1}{2}} \quad \ldots\ldots\ldots\ldots\ldots\ldots \quad 30$$

where the values β_n are the zeros of equation (28).

The effect that the length-to-height ratio has on the natural frequencies is of considerable importance, and

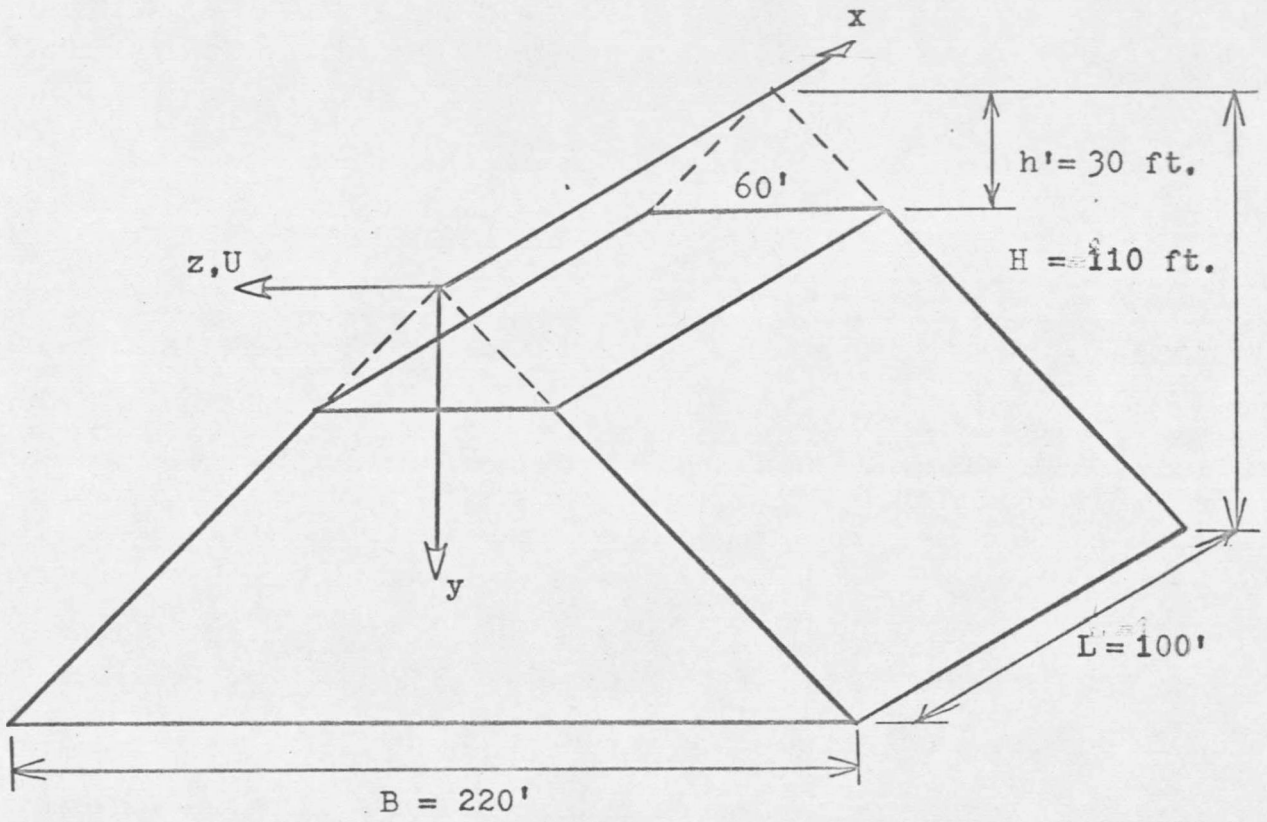


Figure 7: Truncated Shear-Wedge

shear modulus $G = 3.0 \times 10^6$ lbs./ft.^{2}

mass density = 3.0 slugs/ft.^{3}

therefore, a brief discussion of this effect is presented. Ambraseys has shown that the fundamental frequency is essentially independent of length for a length-to-height ratio greater than 3[4]. This can be interpreted from equation (30) to mean $\beta_1^2 \gg (\pi/L)^2$; and therefore, the term (π/L) can be ignored. Although the assumption of an infinite length may give a reasonably good estimate for the fundamental frequency, and a great reduction in the computations, the infinitely long wedge will not provide a reasonable value for the second to the lowest natural frequency. If $\beta_1^2 \gg (\pi/L)^2$ then most probably $\beta_1^2 > (r\pi/L)^2$ where r may be as large as 4 or 5 depending on the magnitude of the actual length-to-height ratio. Thus, the correct second natural frequency is given by

$$\omega_{12} = S\left[\beta_1^2 + \left(\frac{2\pi}{L}\right)^2\right]^{\frac{1}{2}}.$$

For large length-to-height ratios, ω_{12} as well as ω_{13} may be only a few percent above the fundamental frequency, and therefore, of significant importance for computing earthquake response.

The natural frequencies and mode shapes are calculated for the simple structure of Figure 7. A special computer code was programmed to calculate the zeros (β_n) of equation (28), accurate to eight digits. The values β_n are then substituted into equation (30) to obtain the natural frequen-

cies and into equation (29) to obtain the mode shapes.

The natural frequencies obtained from equation (30) are compared with the natural frequencies obtained by the two-dimensional Holzer Method in Table I. As might be expected the finer grid shows better agreement with the continuous system than the coarse grid. It is also worth noting that natural frequencies obtained from the lumped-mass systems are always below the corresponding natural frequencies obtained from the continuous system, with better agreement at the lower frequencies.

The information taken from Table I is helpful in determining an appropriate grid size for an actual problem. If only the first few natural frequencies are of interest, good accuracy can be acheived with a fairly coarse grid of 10 rows and 10 columns. To get good accuracy for higher natural frequencies a finer grid must be used. If at a particular natural frequency the horizontal mode has many node points (r of equation (29) is large) and the vertical mode has only one or two node points (n is small), a large number of columns would then be expected to improve the accuracy of the natural frequencies more than a large number of rows. For the first few natural frequencies of a dam with a large length-to-height ratio, the best accuracy for the least amount of grid refinement is then achieved from a grid with many more columns than

Table I

Comparison of the Natural Frequencies Obtained by a Finite - Element Approximation with the Exact Natural Frequencies for a Truncated Shear-Wedge

frequency designation	exact frequency	finite element approximation. 4 rows x 5 columns		10 rows x 10 columns	
ω_{nr}	(rad./sec)	frequency	% error	frequency	% error
ω_{11}	39.970	39.387	1.46	39.840	.32
ω_{12}	67.517	63.650	5.73	66.543	1.44
ω_{21}	69.014	65.352	5.31	68.391	.90
ω_{22}	87.885	82.286	6.37	86.707	1.34
ω_{13}	97.434	85.507	12.2		
ω_{31}	104.645	89.561	14.4		
ω_{23}	112.510	99.303	11.8		
ω_{32}	117.947	102.573	13.0		
ω_{14}	128.070	98.191	23.4		
ω_{33}	137.282	116.668	15.0		
ω_{24}	139.883	111.180	20.3		
ω_{41}	142.163	103.395	27.2	135.288	4.83
ω_{42}	152.221	114.850	24.5		
⋮	six natural frequencies have been omitted				
ω_{44}	187.123	137.043	26.7	176.475	5.69

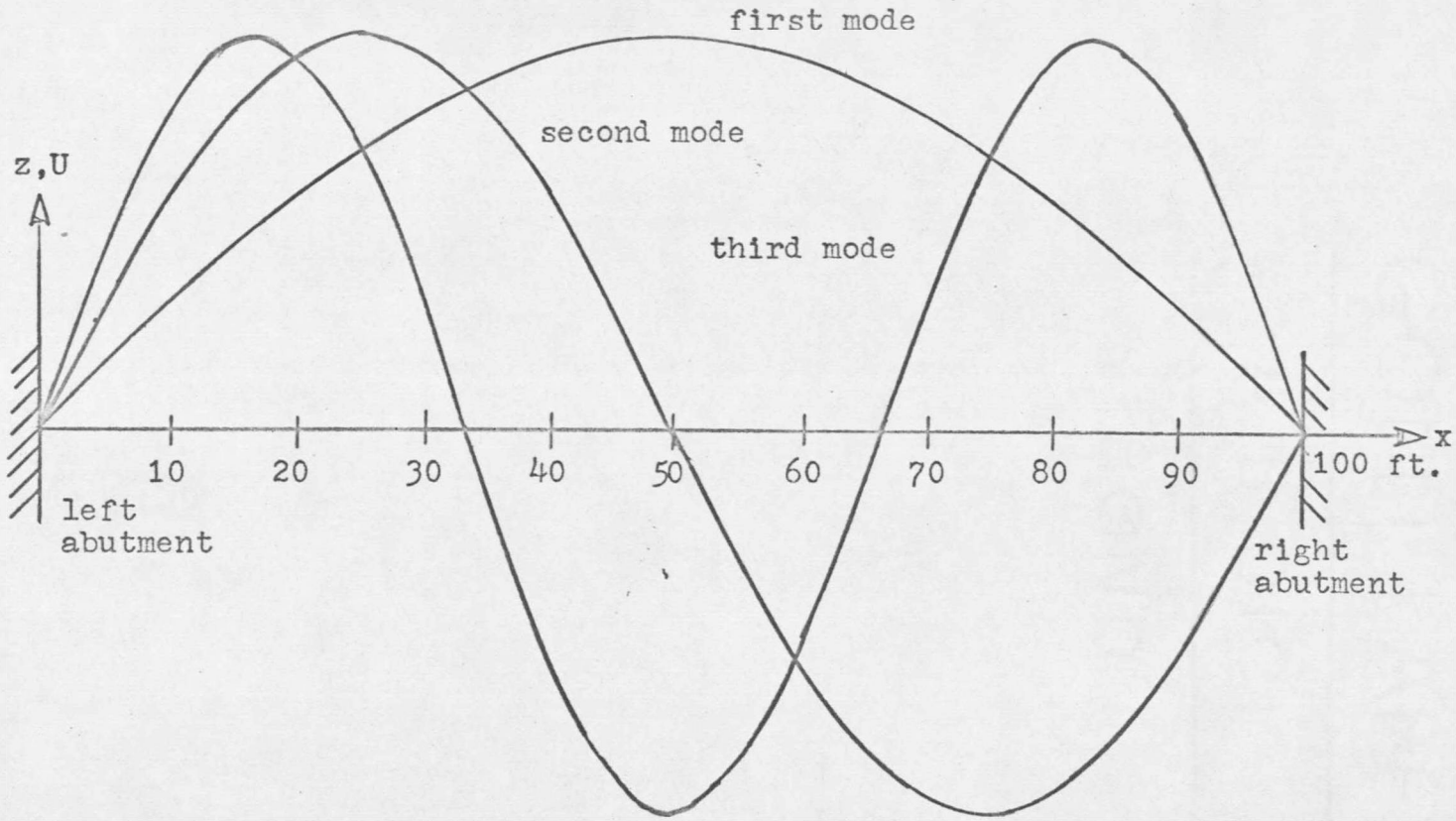
rows. For example the model which is used in the next section for Bouquet Dam consists of a grid with 4 rows and 18 columns.

The first three longitudinal and the first three vertical mode shapes which are calculated from equation (29) are plotted in Figures 8 and 9. Agreement between the mode shapes which are calculated from the numerical grid consisting of 10 rows and 10 columns and the exact mode shapes of equation (29) is within 1% of the maximum displacement of the mode for the first two horizontal modes and the first two vertical modes. It is interesting to note that the longitudinal modes are simple sine waves and the vertical modes are Bessel functions, as is seen from equation (29).

Dynamic Behavior of Bouquet Dam

A check of a different nature is obtained by comparing calculated natural frequencies and mode shapes of an actual dam with the behavior obtained by field measurements. The purpose of this comparison is to provide a knowledge of the effects that the many simplifying assumptions have on the calculated behavior. With this knowledge future analytical investigations can be effectively improved.

A field investigation was conducted by W. O. Keightley[8] to determine the dynamic characteristics of Bouquet Dam, near Los Angeles, California. The major part of the dam, pictured in Figures 10 and 11, consists of a compacted fill of sandy



Plan View

Figure 8: First Three Horizontal Mode Shapes of a Truncated Shear-Wedge

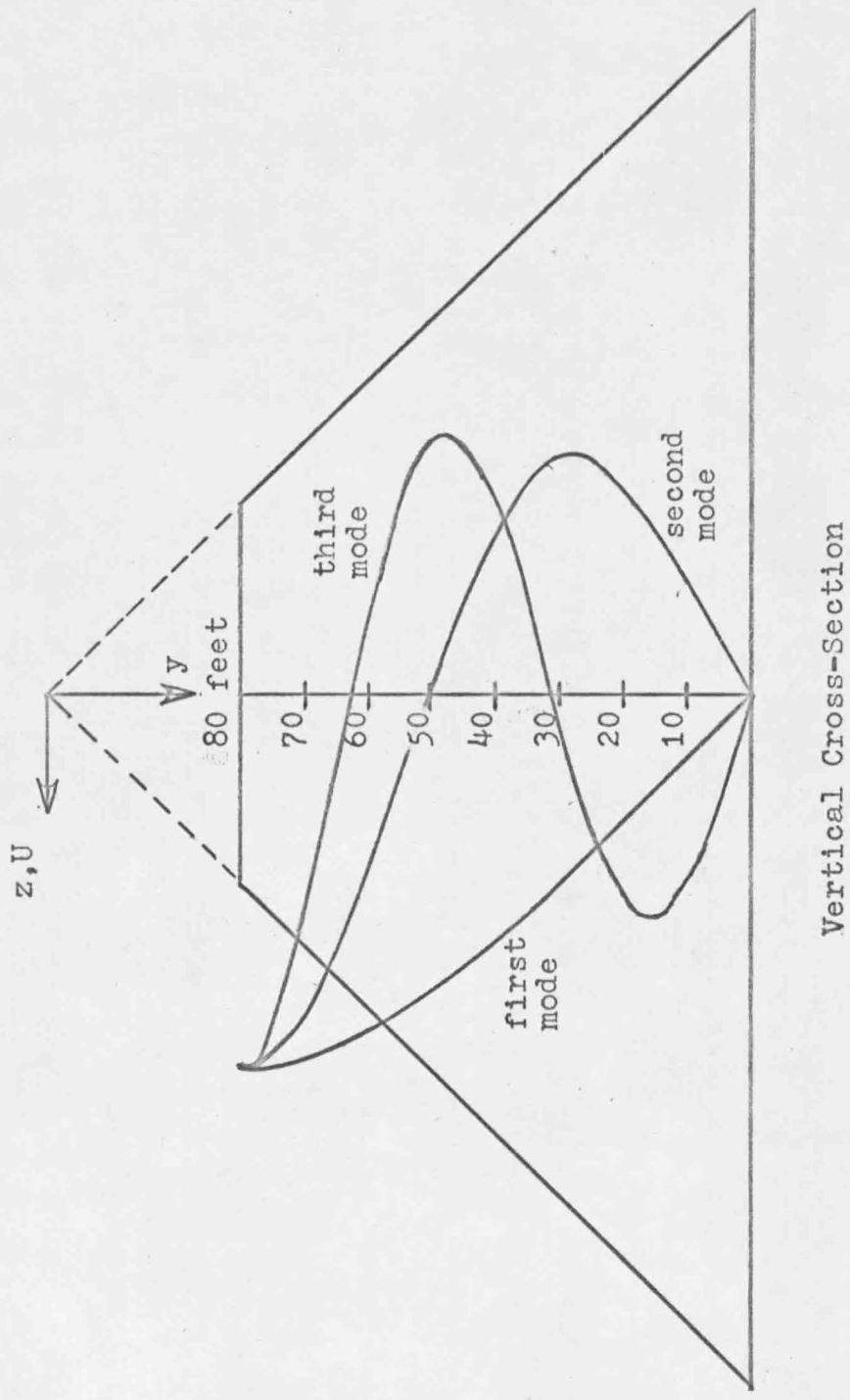
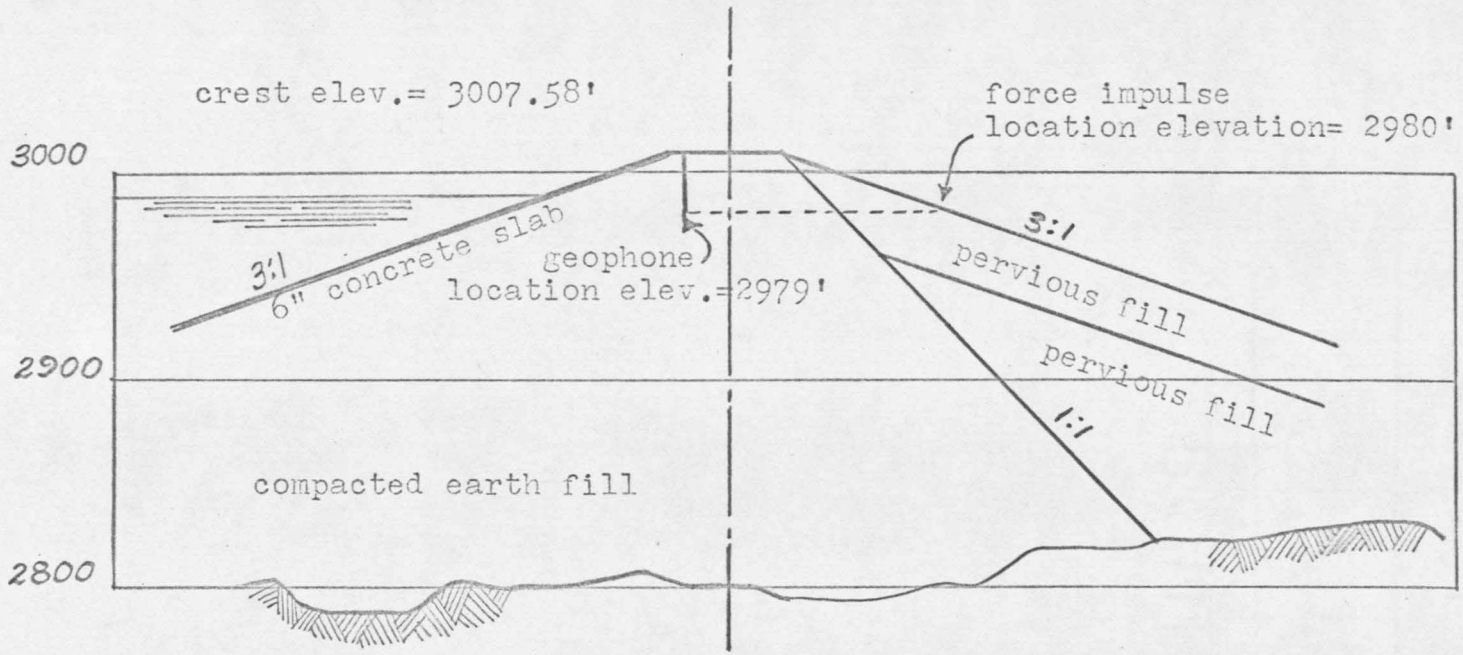


Figure 9: First Three Vertical Mode Shapes of a Truncated Shear-Wedge.

clay. Bouquet Dam differs from the idealized dam in several respects: The fill is not homogeneous; the water content and the overburden pressure both vary with depth, and hence, the elastic properties and the density can be expected to vary with depth. A typical transverse cross section, Figure 10, contains several zones of graded material. Also, the canyon walls are certainly not infinitely rigid as assumed in the theoretical investigation. However, the idealized model does posess some of the major features of the actual dam: The geometry, as seen in an elevation view, is well represented by the grid, shown in Figure 11. Also, the analytical investigation considers only deflections due to shear. It is felt that this is in good agreement with the type of deflections observed on the dam.

A shear wave velocity representative of the entire fill is very difficult to obtain. A shear wave velocity of 1270 feet per second was measured through the thickness of Bouquet Dam at a location about 28 feet below the level of the crest, shown in Figure 10. A force impulse was applied on the downstream face of the dam, thus causing elastic waves to travel through the dam. A geophone, sensitive to motion in only one direction, recorded a signal of the impulse from a location in a vertical well about 132 feet from the point of the impulse. By orienting the sensitive axis of the geophone in a horizon-



Cross-section at Station 7+95

Figure 10. Cross-section of Bouquet Canyon Dam

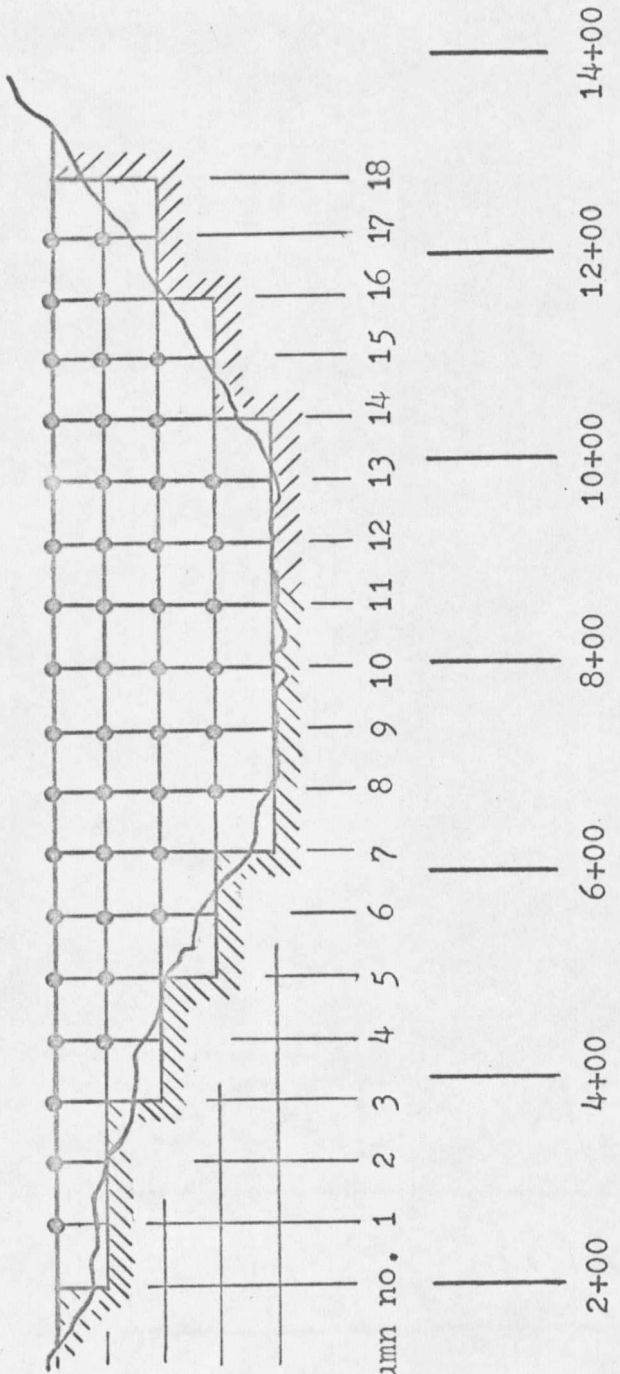


Figure 11: Elevation View of Bouquet Canyon Dam Showing Finite-Element Approximation.

tal direction making an angle of 90° with the source, the travel time for the shear wave was measured, and from this measurement the shear wave velocity of 1270 feet per second was calcuated.

To substantiate the measured shear wave velocity, geophones should be stationed at intermediate distances. This would assure that the motion which was detected by the geophone was actually the shear wave following a straight path from the source and not a reflection of a wave from a plane of discontinuity in the dam. Similar tests show a tendency for the measured shear wave velocity to increase slightly as the magnitude of the force impulse at the source increases, thus placing another degree of uncertainty on the measured shear wave velocity.

Using the measured shear wave velocity of 1270 feet per second and approximating the dam by a grid of 4 rows and 18 columns, shown in Figure 11, the natural frequencies and mode shapes of the dam are calculated. The first six computed frequencies, shown in Table II, are consistantly higher than the observed natural frequencies. The difference increases from a factor of 11% for the first natural frequency to a factor of 25% for the sixth natural frequency.

Due to the uncertainty of the measured shear wave velocity, natural frequencies were also computed using an

Table II

Observed and Computed Natural Frequencies of Bouquet Dam.

Number	Observed	Computed Natural Frequencies			
		Finite-Element Model		Shear-Wedge With Rectangular Boundaries	
		S=1270 fps.	S=1142 fps.	S=1270 fps.	S=1133 fps.
1	2.23 cps.	2.48	2.23	2.50	2.23
2	2.68	3.12	2.81	2.97	2.67
3	3.13	3.71	3.34	3.62	3.14
4	3.62	4.19	3.77	4.34	3.87
5	3.87	4.68	4.21	5.17	4.61
6	4.10	5.12	4.60	5.70	5.08

adjusted shear wave velocity of 1142 feet per second. This adjusted value for the shear wave velocity was chosen to cause the computed fundamental frequency to agree exactly with the observed fundamental frequency. Using the shear wave velocity of 1142 feet per second, and the 4 by 18 grid, the first six computed frequencies are compared with the observed frequencies in Table II. The computed frequencies are again consistently higher than the observed frequencies by 0%, 4.9%, 6.7%, 4.1%, 8.8%, and 12.2% respectively. This indicates that certainly not all of the shortcomings of the analytical method can be attributed to the shear wave velocity.

It is of interest, at this point, to examine the natural frequencies obtained from the exact solution to the differential equation of motion for the idealized dam with rigid vertical ends and a rigid flat bottom, as presented in the previous section. The rectangular boundaries of the shear wedge serve as a crude approximation to the somewhat trapezoidal boundaries of Bouquet Dam, shown in Figure 12. The bottom boundary of the shear wedge is assigned just slightly above the lowest point of the dam thus resulting in a 200 feet high truncated wedge (210 feet high to the apex of the wedge). The ends of the wedge are assigned, without justification, to cause the area of the wedge to be approximately the same as the area of Bouquet Dam as seen in the elevation view of Figure 12. The vertical ends of the rectangular wedge, located in this manner, result in a wedge approximately

Figure 12: Cross-Section and Elevation View of Bouquet Canyon Dam Showing Truncated Shear-Wedge Approximation.

690 feet long.

Using the observed shear wave velocity of 1270 feet per second, the first six natural frequencies of the rectangular wedge are calculated from equation (30) and shown in Table II. Surprisingly, the second and third natural frequencies show better agreement with the observed frequencies than do the second and third natural frequencies which were computed from the more refined finite-element model which fits the irregular boundaries. However, this trend does not continue for the higher natural frequencies. The fourth, fifth, and sixth natural frequencies of the rectangular shear wedge have poorer agreement with the observed frequencies than do the corresponding natural frequencies computed from the finite-element model.

The first six natural frequencies for the rectangular shear wedge are again calculated from equation (30) using an adjusted shear wave velocity of 1133 feet per second. The resulting natural frequencies are higher than the observed frequencies by 0%, -0.4%, +0.3%, 6.9%, 19.1%, and 23.9%.

The main reason for the divergence of the higher natural frequencies of the rectangular wedge from the observed frequencies of the dam is probably due to the crude geometric fit of the somewhat trapezoidal dam by the rectangular wedge. Certainly the two dissimilar geometrics would not be expected

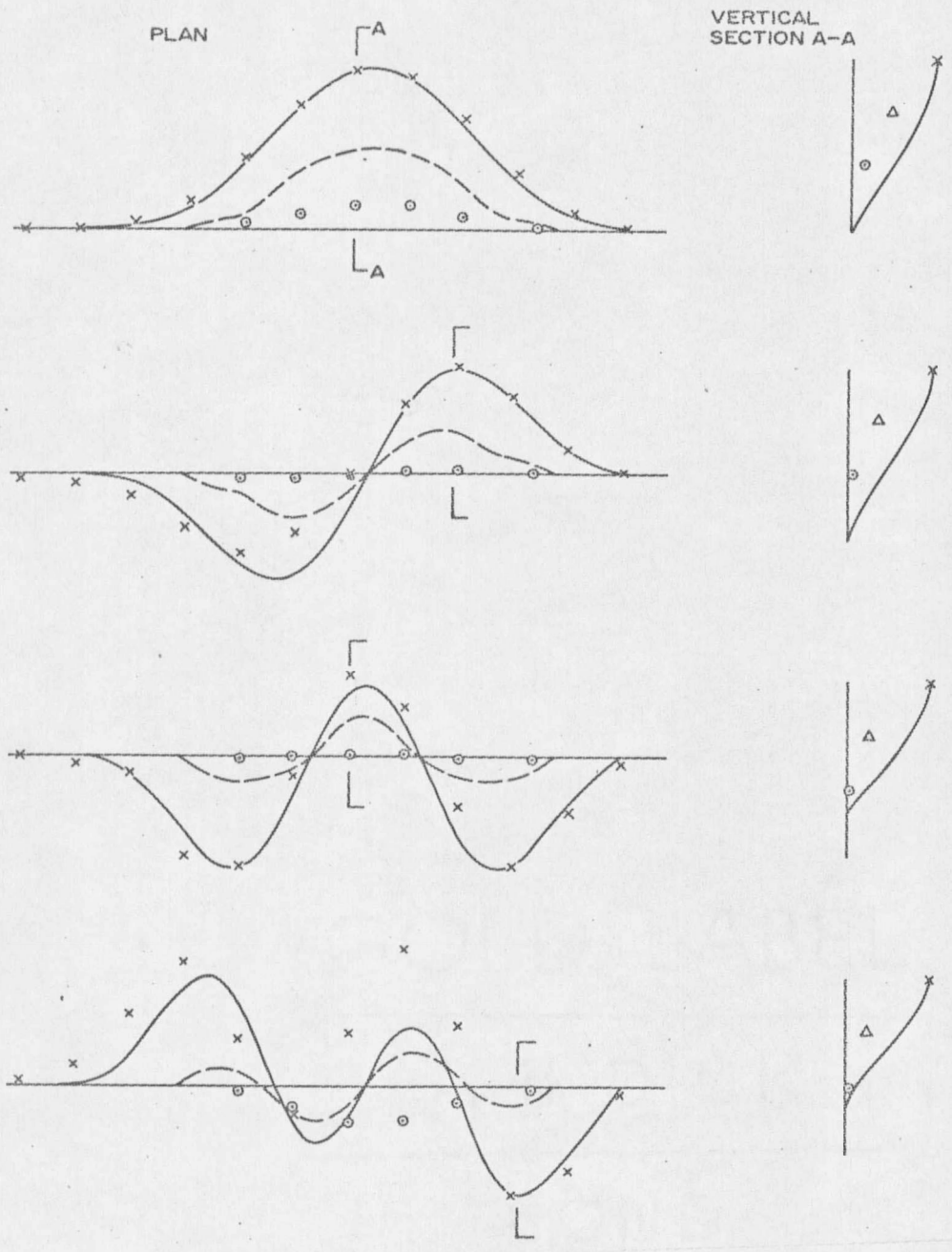
to result in the samenatural frequencies. The adverse effects on the natural frequencies of the rectangular wedge which are caused by the poor geometric fit appear to compensate almost exactly the adverse effects which are caused by all other sources of error in the idealized model for the first three natural frequencies, thus resulting in surprisingly good agreement between the first three computed natural frequencies and the first three observed frequencies. The other sources of error in the idealized model which are referred to in the previous sentence are common with the finite-element model of Figure 11 and are discussed later in this section.

The procedure of choosing a shear wave velocity which causes the computed fundamental frequency to exactly agree with the observed fundamental frequency results in nearly the same wave velocity for the two different idealized models. This fact suggests an interesting and practicable method for measuring the shear wave velocity of an earth dam. Rather than attempting to measure the shear wave velocity directly, perhaps the fundamental frequency could be measured more accurately and with less effort. A good estimation of the shear wave velocity could then be determined from an analytical method such as the one described here. It appears that even the rectangular wedge approximation of the dam could result in a good estimation of the shear wave velocity in this

manner.

The computed mode shapes of the finite-element model are compared with the observed mode shapes of the dam in Figure 13. The computed mode shapes are normalized to cause the maximum computed deflection to agree with the maximum observed deflection for each mode. The figure shows measured deflection at three levels on the downstream face of the dam. Line C is located about four tenths of the distance from the base to the crest, and line B is located about seven tenths of the distance from the base to the crest.

The computed shape of the crest shows surprisingly good agreement with the observed shape for the first mode. The second, third, and fourth computed modes exhibit the same general patterns as the observed modes with the fourth mode having the poorest agreement. Not all of the lack of agreement is attributed to the deficiencies of the analytical work. The observed mode shapes may contain errors as the result of difficulties which are encountered in attempting to measure pure mode shapes experimentally. Also worth noting are the small deflections which were observed near the ends of the crest due to the elastic compliance of the canyon walls. Assuming that the observed deflections are reliable for these extremely small measurements, the largest displacement of the abutments at the level of the crest is



OBSERVED MODE SHAPES

× crest
△ line B
⊙ line C

COMPUTED MODE SHAPES

——— crest and sections
----- line C

Figure 13: Computed Mode Shapes Compared with Observed Mode Shapes.

about 7½% of the maximum displacement of the crest for the fourth mode.

Looking at the cross-section of the dam, also shown in Figure 13, the observed shape shows poor agreement with the computed shape. Much smaller deflections were observed in the lower regions of the dam than were calculated. The appearance of the observed vertical mode shapes might lead one to believe that bending deflections play a major role in the vibrational behavior of the dam. Certainly bending deflections have some effect on the behavior of a dam, but, as discussed earlier in Chapter II, it is felt that the bending deflections are very small compared to the shear deflections.

The most probable reason for the large errors in the calculated deflections at the lower regions of the dam stems from an assumption which was made to simplify the analytical procedure. It was assumed that there is no relative movement of points through the thickness of the dam. This assumption allowed the mass through the thickness to be collapsed into concentrated elements of mass, thus forming the grid of Figure 11. The calculated deflections actually represent the average deflections, of the entire cross-section. The observed deflections, on the other hand, were measured on the downstream face of the dam. The question then arises: Should the two deflections, which are of a slightly different nature,

be expected to agree?

According to Chopra and Clough in their recent report on "Earthquake Response of Homogeneous Earth Dams",(9) considerable differences in the deflections of the centerline of the cross-section and the face of the dam should be expected, at least for the fundamental mode. The vibrations in the plane of the cross-section of an infinitely long dam with side slopes 3:1 (same as Bouquet Dam) have been computed. The results indicate that the centerline may have horizontal deflections which are more than twice as great as the deflections of the two faces of the dam for the fundamental mode. This information appears to explain the excessively large computed deflections in the lower regions of the dam.

Many simplifying assumptions were made to reduce the complicated three-dimensional earth dam to an idealized two-dimensional lumped-mass system. Some of the major reasons that the behavior of the idealized mathematical model does not exactly agree with the behavior of an actual dam are as follows:

1. Reliable soil characteristics of the dam are not readily available. The effect of the shear wave velocity on the natural frequencies is seen in Table II.

2. The dam is not actually homogeneous as assumed in the analytical investigation. A method which can treat

variations in soil characteristics throughout the dam is described later in the chapter titled "Recommendations for Future Work".

3. All bending deflections have been ignored in the idealized model. As discussed earlier in Chapter II, Motohiro Hatanaka[3] estimates the fundamental frequency will be too large by about 2.2% due to neglecting bending deflections. An investigation which is being conducted to include the effects of bending as well as shear is discussed in the chapter titled "Recommendations for Future Work".

4. The observed mode shapes show sizeable deflections of the canyon walls which were assumed to be rigid in the idealized model. Preliminary work, not included in this paper, indicates that the natural frequencies should reduce by no more than about 3% if the elastic compliance of the boundaries is included in the study.

5. The stresses introduced by the sinusoidal force applied to Bouquet Dam were very small and therefore well within the linear range[8]. However, damping does exist which could cause the observed behavior to differ slightly from the undamped computed behavior. The effects that damping have on the mode shapes are

difficult to define. Modal damping is, of course, assumed to represent suitably the effects of damping on the actual structure as discussed earlier in Chapter III.

6. Probably most important of all, the vibrating physical dam is actually a three-dimensional phenomenon. Each point in a vibrating dam will, in general, have three components of motion, and the motion of each component is dependent on the motion of the other two components as a result of Poisson's effect. Thus, the idealized two-dimensional approach explained in this paper can never be expected to predict the total behavior of an earth dam during an earthquake. However, some of the major features of the vibrational behavior of an actual dam can be predicted, and perhaps the method will be capable of predicting response which is quite representative of the actual behavior of an earth dam if the method is further refined as discussed in the section titled "Refinements of the Model".

Chapter V

SUMMARY AND CONCLUSIONS

Summary

An analytical method for calculating some of the major features of the vibrational behavior of an earth dam is presented. The dam is considered to consist of a homogeneous fill situated in a rigid canyon with an arbitrary cross section. Vibrations are restricted to motion in the direction transverse to the longitudinal axis, with no relative motion through the thickness of the dam.

A numerical solution for the idealized dam is presented. The continuous system is replaced by a finite-element system which is composed of a grid of point masses interconnected by shear-resistant springs. The natural frequencies and mode shapes of this two-dimensional system are computed by an iterative technique which is an extension of the Holzer Method for one-dimensional vibrating systems.

Natural frequencies and mode shapes are calculated for a dam located in a rigid canyon with a rectangular cross-section. The frequencies and mode shapes thus obtained are compared with natural frequencies and mode shapes determined from the exact solution to the differential equation of motion. The fundamental frequency calculated by the two-dimensional Holzer Method is 1.46% below the exact fundamental frequency,

when a coarse grid of 4 rows and 5 columns is used, but it is only 0.33% below the exact fundamental frequency, when a finer grid of 10 rows and 10 columns is used. Larger differences between the numerical and the exact natural frequencies are observed for higher modes of vibration. The twentieth natural frequency is 26.7% below the exact value when the grid consists of 4 rows and 5 columns. This error in the twentieth natural frequency is reduced to 5.7% when the finer grid with 10 rows and 10 columns is used.

The mode shapes of the finite-element model show good agreement with the mode shapes of the continuous model which are expressed in terms of trigonometric and Bessel functions. The maximum error in the first two horizontal modes and the first two vertical modes is less than 1% of the largest deflection in the mode when the grid with 10 rows and 10 columns is used.

Calculated natural frequencies and mode shapes for Bouquet Dam are compared with the natural frequencies and mode shapes observed in a field investigation. The lowest six computed natural frequencies, using the unsubstantiated shear wave velocity measured on the dam of 1270 feet per second, are consistantly higher than the observed natural frequencies. The difference increases from a factor of 11% for the first natural frequency to a factor of 25% for the sixth natural frequency.

The computed mode shapes, which are meant to be representative of the entire cross-section, are compared with the observed mode shapes which were measured on the downstream face of the dam. The computed deflections of the crest show the same general shape as the observed deflections with surprisingly good agreement for the first mode. The computed deflections are more than twice as large as the observed deflections in the lower regions of the dam. This discrepancy is attributed to the strains through the thickness of the dam which were ignored in the analytical investigation. Recent work by Chopra and Clough[9] indicates that the deflections of the vertical axis of the cross-section are much larger than the deflections of the two faces of the dam for the lower regions of the dam. This behavior causes the computed deflections (representative of the integrated average of all the deflections through the thickness) to be larger than the observed deflections which were measured on the downstream face of the dam.

A method for determining the shear wave velocity of an earth dam is proposed. The fundamental frequency of the dam is experimentally measured. An analytical investigation then locates the shear wave velocity which causes the computed fundamental frequency to exactly agree with the observed fundamental frequency, thus obtaining a good estimation of

the effective shear wave velocity, representative of the entire dam. The accuracy of the shear wave velocity determined in this manner would then depend on the sophistication of the analytical method. Although the analytical method described in this paper can not fully explain the behavior of a vibrating earth dam, the method is sufficiently reliable to obtain a good estimation of the shear wave velocity. The knowledge of this shear wave velocity then allows for the determination of the higher natural frequencies and modes of vibration.

A method is also presented for calculating linear response of the idealized dam subjected to an arbitrary boundary disturbance. The method is general enough to include the effects of a traveling wave which causes nonrigid boundary motion. Solutions to sample problems have been obtained using this method, but they have not been substantiated by an independent method, and for this reason they are not presented in this paper. A method for verifying the solutions is suggested in Appendix C.

Conclusions

The exact behavior of an earth dam cannot be computed from a two-dimensional model. Approximating the dam by a two-dimensional model is not an attempt to avoid facing up to this fact, but rather the two-dimensional approximation

serves as a stepping stone to the very difficult three-dimensional problem. Two-dimensional techniques can also offer a reasonably good understanding of the vibrational behavior of an earth dam for the purpose of improving designs as well as guarding against possible catastrophic failures.

If a two-dimensional approximation of the dam is to be used for the purpose of simplifying the analytical method, the question then arises: Which two-dimensional model can more closely represent the behavior of an actual dam? The model used for this investigation, which ignores vibrations through the thickness of the dam, is certainly one candidate for the job.

Another feasible two-dimensional model is obtained by considering an infinitely long dam. The vibrations in the plane of the cross-section, in both the horizontal and the vertical directions, can then be determined from this idealized model. The one outstanding advantage of this approach is the direct relationship between the stresses in the plane of the cross-section and one very plausible mechanism for failure. If a sloughing of the earth on one of the faces of the dam is considered a likely cause for failure of the dam, the knowledge of the stresses in the plane of the cress-section will certainly offer considerable insight of the failure of the dam.

The method of representing a dam by an infinitely long model appears to be representative of the behavior of an actual dam for the first mode of vibration, but the method does not offer reasonable values for the higher natural frequencies and mode shapes. This fact can be verified by substituting an infinite value for L into the equations (29) and (30) as discussed earlier. For example, if the length of the truncated wedge approximation of Bouquet Dam, shown in Figure 12, is extended to infinity, the first six natural frequencies are above the observed frequencies by 4.5%, 101.%, 175.%, 224.% 283.%, and 339.% respectively. Also the higher modes computed from an infinitely long model do not resemble the shapes of the observed modes.

The two-dimensional model described in the paper, on the other hand, results in natural frequencies and mode shapes which show good agreement with the observed behavior. However, the computed shear stresses on planes perpendicular to the longitudinal axis of the dam do not appear to be directly related to a likely mechanism for failure.

Perhaps the knowledge of the transverse accelerations of the dam, obtained from the two-dimensional model described in this paper, can be related to the mechanism for failure in which a mass of earth sloughs off from the upstream or downstream face of the dam in a future investigation. At any

rate, an important step toward understanding the behavior of a vibrating earth dam is being taken. This step is completed when an analytical method is developed that can predict the behavior of an actual dam at low levels of stress with good reliability. The next step will then be to predict the behavior of a dam at levels of stress approaching failure.

Chapter VI

RECOMMENDATIONS FOR FUTURE WORK

Refinements of the Model

In addition to the need for investigating other methods for calculating the dynamic behavior of structures, there is a need for further development of the finite-element approach used in this paper. An idealized model is established to represent the actual dam in as many ways as possible without complicating the analytical method for calculating the behavior of the model beyond the limit of feasibility. Many simplifications were made to arrive at the two-dimensional model used in this report. Future work can predict behavior which will more nearly represent the behavior of an actual dam if a more refined model is used. A few suggested refinements of the model are cited below:

1. Due to insufficient knowledge of the actual soil characteristics, the dam has been treated as a homogeneous fill. If the actual soil characteristics are known at each point of the dam, the two-dimensional representation can allow for variations of the soil characteristics in the plane of the grid. This refinement will prove particularly beneficial for varying soil characteristics in the vertical direction to account for

variations in the water content of the soil and in the overburden pressure with depth. It should be noted, however, that the soil characteristics assigned to each point in the grid is actually an integrated average of the characteristics through the thickness of the dam.

2. The finite-element approximation of the dam is sufficiently general to allow for an irregularly shaped end abutments as well as a non-symmetric cross-section. The finite-element model can be further refined to allow for a non-linear taper of the faces of the dam. This refinement will prove beneficial for representing an earth dam with a variable taper, as is often the case. Figure 12 shows that the face of Bouquet Dam actually changes slope near the bottom of the dam, although this dam was represented in the analytical investigation by a model with a linear taper over the entire height.

3. Bending deflections are considered small in comparison to the shear deflections for an earth dam with a large ratio of base thickness to height. A better representation of a dam, particularly a dam with steep side slopes, can be achieved by analyzing a model which includes the effects of bending. In other words the dam is represented by a thick plate with a variable thickness. A

model for a thin plate is described in a recent paper by A. L. Yettram and H. M. Husain[10]. Mr J. K. Khanna, a graduate student in Civil Engineering at Montana State University, is presently engaged in an investigation which utilizes this model to include the effects of bending as well as shear in the analysis of an earth dam.

4. Additional knowledge about the vibrational behavior of a dam can be gained from an analytical study which includes vibrations in the plane of the two-dimensional grid. This more refined model would also permit the analysis of a dam which has a bend in the longitudinal axis. C. W. McCormick[11] has described a model, consisting of a rectangular grid of point masses interconnected by straight elastic members which is capable of representing both dilatational and shear distortions in the plane of the grid. Another model for calculating vibrations in the plane of the grid has been presented by R. W. Clough[12].

Analyzing a dam with a bend in the crest would complicate the analytical method considerably. At each point where the longitudinal axis bends, the motion which is transverse to the plane of the grid on one side of the bend has components in both the transverse direction and the longitudinal direction on the other side of the bend.

Hence, in-plane vibrations must be studied as a preliminary step to analyzing a dam with a bend in the longitudinal axis.

5. Due to the complex nature of the compliance of the foundation under a structure, the foundation is generally considered to be infinitely rigid or else the foundation is assumed to consist of a system of elastic springs. An approximation to the compliance of the abutments of the dam can be accomplished by placing a spring at each point on the boundary of Figure 2 where a shear spring of the finite-element model attaches to the rigid boundary. Preliminary work to approximate the foundation compliance in just this manner indicates that the two-dimensional Holzer Method, used to calculate the natural frequencies and the mode shapes of the grid, is only slightly more complicated with elastic boundaries than with rigid boundaries. The major difficulty encountered is in determining the proper spring constant to assign to each spring along the boundary.

6. The physical dam dissipates energy internally as a function of strain, and it radiates energy externally as a function of the amplitude of the boundary motion. For low levels of strain, the structure is well repre-

sented by a mass-spring grid with viscous dashpots connected from each mass point to a rigid support and from each mass point to every other mass point. Even if a method for determining the dashpot coefficients which would best represent the dam could be found, calculating the dynamic behavior of the grid would be rather difficult. If the damping results in motion at a natural frequency in which all the points are moving in phase, the configuration of damping is referred to as modal damping. The use of a configuration of damping other than the modal damping which is used in this investigation will complicate the analysis considerably.

At higher levels of strain, the viscous dashpot method of representing the internal energy dissipation cannot be justified. Excessive strain causes sliding between individual soil particles, thus introducing an energy dissipation known as Coulomb or hysteretic damping. When this occurs the system is no longer linear, and the method of calculating response by superimposing modes is no longer valid. Each spring constant of the mass-spring grid now depends on the state of stress and strain and on the past history of strain.

A general method for computing this nonlinear response is discussed earlier in Chapter II. The solution proceeds by numerically integrating the equations of motion for each point mass over small intervals of time. Although the method is applicable at high levels of stress where failure is imminent, computing problems may arise for motion which continues for just a few seconds as the result of the large number of calculations which are required and the cumulative nature of the errors. Perhaps the problem of stability can be remedied by computing response by means of a less rigorous linear method until nonlinearities just start to occur, and then the more general method which is applicable for high levels of stress can be used to continue the solution into the nonlinear response where stresses are critical. Computing response at high levels of stress will require a major revision in the techniques used in this investigation.

APPENDIX

APPENDIX A

Differential Equation of Motion for a Shear Dam

The element of earth through the thickness of the dam, shown in Figure 14, is considered. Ignoring relative deflections through the thickness of the dam, the differential equation of motion is obtained by summing the forces on the element:

$$\rho \, dx \, dy \, z \, \frac{\partial^2 U}{\partial t^2} = \frac{\partial V_v}{\partial x} dx + \frac{\partial V_h}{\partial y} dy \qquad \text{.....} \quad 31$$

where z is the thickness of the dam, ρ is the mass density, U is the transverse deflection of the element, V_v is the total force on the vertical face of the element, and V_h is the total force on the horizontal face of the element. The forces on the element are related to strain by Hooke's law as follows:

$$V_v = A_v G \frac{\partial U}{\partial x} = z \, dy \, G \frac{\partial U}{\partial x}$$

$$V_h = A_h G \frac{\partial U}{\partial y} = z \, dx \, G \frac{\partial U}{\partial y} .$$

Substituting these values for V_v and V_h into equation (31) gives the general equation of motion in terms of displacement:

$$\frac{\partial}{\partial x}\left[z \, G \frac{\partial U}{\partial x}\right] + \frac{\partial}{\partial y}\left[z \, G \frac{\partial U}{\partial y}\right] = z \rho \frac{\partial^2 U}{\partial t^2} . \qquad \text{....} \quad 32$$

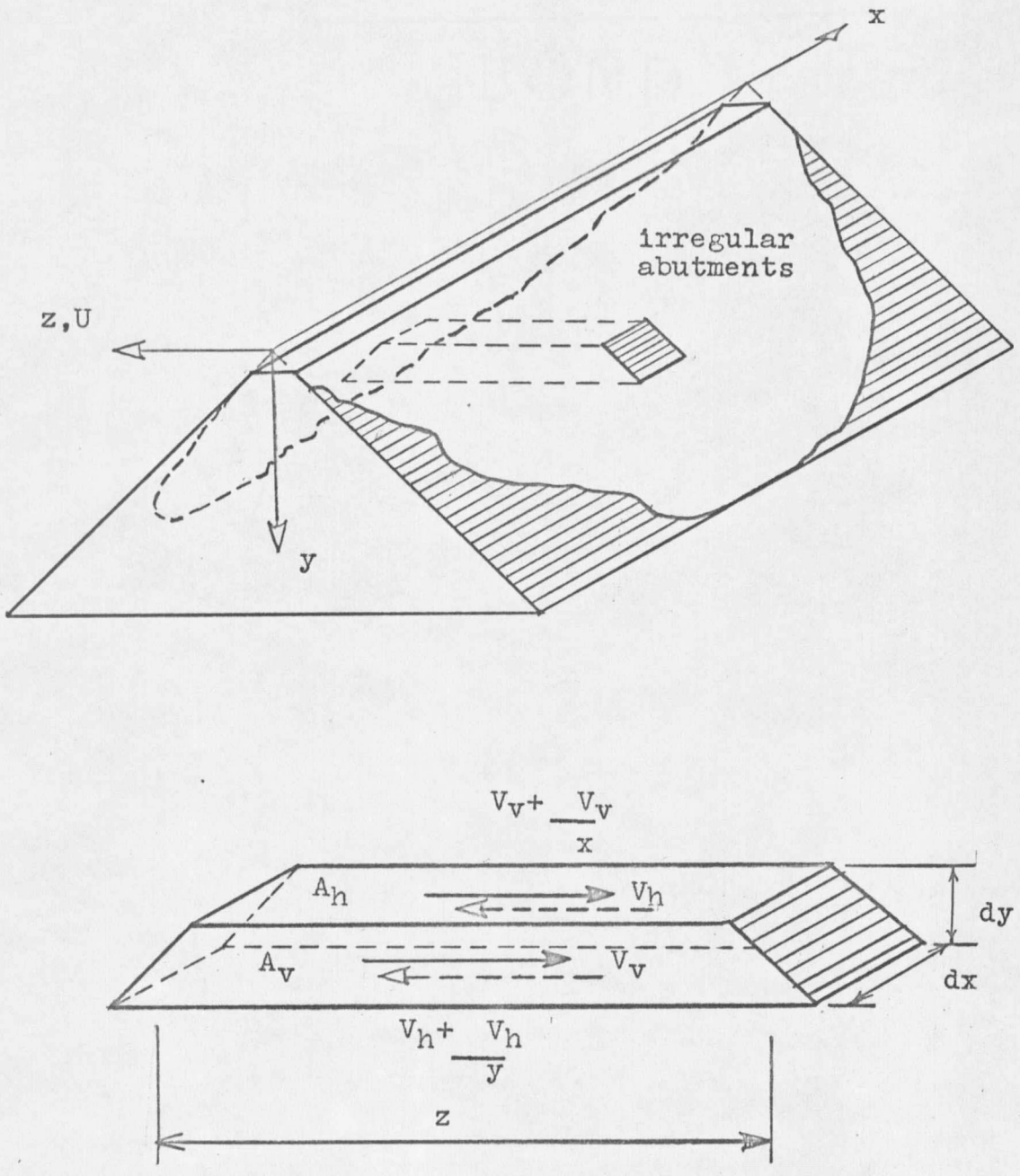


Figure 14: Infinitesimal Element of Soil Extending Through the Dam.

If the dam has a linear taper, z can be replaced by cy where c is a constant, and if the dam is homogeneous, G can be taken outside the partial derivative operator and the equation of motion becomes:

$$\frac{G}{\rho}\left[\frac{\partial^2 U}{\partial x^2} + \frac{\partial^2 U}{\partial y^2} + \frac{1}{y}\frac{\partial U}{\partial y}\right] = \frac{\partial^2 U}{\partial t^2} . \qquad \text{.....} \quad 33$$

APPENDIX B

Orthogonality of the Modes of Vibration of a Shear Dam

If the transverse deflection U(x,y,t) is of the form:

$$U(x,y,t) = F(x,y)\ T(t)$$

$$= F(x,y)\ \text{Sin}\ (\omega t - \alpha)\ ,$$

then equation (32) of Appendix A can be written:

$$\frac{\partial}{\partial x}\left[z\ G\ \frac{\partial F}{\partial x}\right] + \frac{\partial}{\partial y}\left[z\ G\ \frac{\partial F}{\partial y}\right] = -z\rho\omega^2 F\ .$$

If $\omega = \omega_n$, the n^{th} natural frequency, then F(x,y) becomes the n^{th} mode shape Φ_n i.e.

$$\frac{\partial}{\partial x}\left[z\ G\ \frac{\partial \Phi_n}{\partial x}\right] + \frac{\partial}{\partial y}\left[z\ G\ \frac{\partial \Phi_n}{\partial y}\right] = -z\rho\omega_n^2\ \Phi_n \qquad \ldots\ldots 34$$

similarly,

$$\frac{\partial}{\partial x}\left[z\ G\ \frac{\partial \Phi_m}{\partial x}\right] + \frac{\partial}{\partial y}\left[z\ G\ \frac{\partial \Phi_m}{\partial y}\right] = -z\rho\omega_m^2\ \Phi_m\ . \qquad \ldots\ 35$$

Equation (34) is multiplied through by $\Phi_m \frac{dV}{z}$ and integrated over the volume, similarly equation (35) is multiplied through by $\Phi_n \frac{dV}{z}$ and integrated over the volume. The resulting integral equations are then subtracted giving:

$$+\int_{\text{Vol.}} \frac{\Phi_m}{z}\left\{\frac{\partial}{\partial x}\left[z\,G\,\frac{\partial \Phi_n}{\partial x}\right]+\frac{\partial}{\partial y}\left[z\,G\,\frac{\partial \Phi_n}{\partial y}\right]\right\} dV \;+$$

$$-\int_{\text{Vol.}} \frac{\Phi_n}{z}\left\{\frac{\partial}{\partial x}\left[z\,G\,\frac{\partial \Phi_m}{\partial x}\right]+\frac{\partial}{\partial y}\left[z\,G\,\frac{\partial \Phi_m}{\partial y}\right]\right\} dV \;=$$

$$+\int_{\text{Vol.}} (\omega_m^2-\omega_n^2)\,\rho\,\Phi_n\,\Phi_m\,dV\;. \qquad \ldots\ldots\ldots\ldots\ldots\ldots \quad 36$$

The left side is expanded by substituting $dV = z\,dx\,dy$ and integrating by parts on x and y as appropriate, i.e.:

$$+\int_{y} z\,G\,\Phi_m\,\frac{\partial \Phi_n}{\partial x}\,\Big|_{\text{evaluated over x}}\,dy \;-\int_{\text{Vol.}} z\,G\,\frac{\partial \Phi_m}{\partial x}\frac{\partial \Phi_n}{\partial x}\,dx\,dy$$

$$+\int_{x} z\,G\,\Phi_m\,\frac{\partial \Phi_n}{\partial y}\,\Big|_{\text{evaluated over y}}\,dx \;-\int_{\text{Vol.}} z\,G\,\frac{\partial \Phi_m}{\partial y}\,\frac{\partial \Phi_n}{\partial y}\,dx\,dy$$

$$-\int_{y} z\,G\,\Phi_n\,\frac{\partial \Phi_m}{\partial x}\,\Big|_{\text{evaluated over x}}\,dy \;+\int_{\text{Vol.}} z\,G\,\frac{\partial \Phi_n}{\partial x}\,\frac{\partial \Phi_m}{\partial x}\,dx\,dy$$

$$- \int_x z\, G\, \Phi_n \frac{\partial \Phi_m}{\partial y} \Bigg|_{\text{evaluated over } y} dx + \int_{\text{Vol.}} z\, G \frac{\partial \Phi_n}{\partial y} \frac{\partial \Phi_m}{\partial y}\, dx\, dy.$$

This expanded form is simplified by noting that the second term and the sixth term cancel, also the fourth term and the eighth term cancel. The first and fifth terms vanish since Φ_m and Φ_n are zero all along the limits on x, i.e. the deflections at the end abutments is zero. The third and seventh terms vanish at the upper limit on y, because Φ_m and Φ_n are both zero all along the bottom boundary of the dam. The lower limit on y also vanishes in the third and seventh terms, because the shearing strain, $\frac{\partial \Phi}{\partial y}$, is zero all along the crest. Thus, the entire left side of equation (36) vanishes, giving the desired form:

$$(\omega_m^2 - \omega_n^2) \int_{\text{Vol.}} \rho\, \Phi_m\, \Phi_n\, dV = 0.$$

for $m \neq n$, then $\omega_m^2 \neq \omega_n^2$ and

$$\int_{\text{Vol.}} \rho\, \Phi_m\, \Phi_n\, dV = 0.$$

APPENDIX C

Proposed Verification of Mode Superposition Calculations

The calculations for general response, using the method of superimposing mode shapes, need verification by an independent method. An independent method is proposed for the special case of calculating steady-state response resulting from sinusoidal boundary motion. The same mass-spring model, shown in Figure 2, with irregular boundaries, is used for both methods. The more general superposition method is to be checked by comparing the response of a particular dam to a sinusoidal boundary disturbance, calculated by the superposition method, with the response calculated by the steady-state method.

The steady-state method for calculating response does not make use of natural frequencies and mode shapes. When the boundaries of Figure 2 experience steady-state sinusoidal motion at the frequency ω, each of the internal mass points is also vibrating at the frequency ω. When the points along the boundaries have sinusoidal motion but are not moving in phase with each other, each internal mass point is still vibrating at the frequency ω, but in general it will not be moving in phase with its neighboring points. Thus, the motion of the particular mass point (i,j) is given by

$$U_{i,j}(t) = A_{i,j} \operatorname{Sin} (\omega t - \alpha_{i,j}),$$

where $A_{i,j}$ is the amplitude of displacement of the point (i,j), and the phase angle $\alpha_{i,j}$ is the angle by which point (i,j) lags some reference point, say the extreme left of the crest. The phase angle α is introduced to allow for nonrigid boundary motion in which points along the boundaries are not moving in phase, and it should not be misinterpreted as an indication of damping. The accelerations of each mass-point can then be expressed:

$$\ddot{U}(t) = -\omega^2 U(t)$$

regardless of the phase angle α.

The left and bottom boundary points of Figure 4(a) are assigned the deflected shape assumed by the boundaries at a designated time t_o. The right boundary is temporarily free. A zero shear force is assigned to each of the horizontal shear strings on the extreme left of the grid, and the right boundary deflections, $\{U^{(1)}\}$, are calculated by the step-by-step procedure previously described*. The right boundary displacements $\{U^{(2)}\}$, of Figure 4(a) have been expressed previously as a linear combination of left boundary shears in equation (7) with the left and bottom boundary points assigned zero displacement. The right boundary displacements $\{U^{(1)}\}$, due

---

* Although the Holzer Method has customarily been applied to systems in which all points are vibrating in phase, careful study of the equations show that they are applicable also to systems in which all points are vibrating at one frequency, but not necessarily in phase.

to left and bottom boundary displacements, when added to the right boundary displacements $\{U^{(2)}\}$, due to the left boundary shears, must give the actual displacements $\{U^{(a)}\}$ assumed by the right boundary points at the designated time t_o, thus:

$$\{U^{(1)}\} + \{U^{(2)}\} = \{U^{(a)}\} .$$

But

$$\{U^{(2)}\} = [C] \{V\}$$

from equation 7, so the preceding equation can be written:

$$\{V\} [C] = \{U^{(a)}\} - \{U^{(1)}\} . \quad \text{.....} \quad 37$$

The left boundary shears $\{V\}$ are calculated from equation (37) since both $\{U^{(a)}\}$ and $\{U^{(1)}\}$ are known. The total internal shear forces and deflections are then calculated by the step-by-step procedure of working across the grid from left to right.

A brief time later the boundaries assume a slightly different distorted shape from which a new set of internal shear forces and deflections are calculated. Response, calculated in this manner at many different time intervals over one cycle of boundary motion, gives a complete picture of the displacement response of the dam.

The displacement response of the same grid experiencing the same sinusoidal disturbance is then calculated by superimposing mode shapes. Even though the boundary disturbance

is sinusoidal, the solution obtained by this method has a transient component. The dam is initially at rest, and several cycles of boundary motion are required for the motion of the dam to reach a steady-state condition, depending on the amount of modal damping that is assumed. If no modal damping is included, the response never reduces to a steady-state condition. On the other hand, if considerable modal damping is assumed, the calculated response would necessarily show poor agreement with the undamped response calculated by the steady-state method, particularly at frequencies near a natural frequency for the system.

The introduction of modal damping to reduce the transient response to steady-state response can offer only a qualitative comparison of the two methods, which may not be very conclusive. A conclusive quantitative comparison can be accomplished, however, by altering the superposition method slightly. The proper initial conditions, as determined by the steady-state solution, are assigned to each mass-point, and the response due to the sinusoidal boundary motion is then calculated by the superposition method, with no modal damping. If the total response of the dam, resulting from the initial conditions and the boundary motion, agrees with the response determined by the steady-state method, a quantitative check has been accomplished.

LITERATURE CITED

1. Hildebrand, F. B., Methods of Applied Mathematics, Prentice-Hall Inc., Englewood Cliffs, N. J., (1960), pp. 227-345.

2. Jacobsen, Lydik S., and Ayre, Robert, Engineering Vibrations, McGraw-Hill, New York, N. Y., (1958), pp. 104-110.

3. Hatanaka, Motohiro, "Fundamental Considerations on the Earthquake Resistant Properties of the Earth Dam", Disaster Prevention Research Institute, Bulletin No. 11, Kyoto, Japan, (December, 1955).

4. Ambraseys, N. N., "On the Shear Response of a Two-Dimensional Truncated Wedge Subjected to an Arbitrary Disturbance," Bulletin of the Seismological Society of America, Vol. 50, (January, 1960), pp. 45-56.

5. Holzer, H,. Die Berechnung der Drehschwingungen, Springer-Verlag, Berlin, 1921.

6. Myklestad, N. O., "A New Method of Calculating Natural Modes of Uncoupled Bending Vibration of Airplane Wings and Other Types of Beams," Journal Aero. Sci., (April, 1944), pp. 153-162.

7. Prohl, M. A., "A General Method for Calculating Critical Speeds of Flexible Rotors," Journal of Applied Mechanics, (September, 1945).

8. Keightley, W. O., "A Dynamic Investigation of Bouquet Canyon Dam," Earthquake Engineering Research Laboratory, California, (September, 1964).

9. Chopra, Anil K., Clough, Ray W., "Earthquake Response of Homogeneous Earth Dams," Soil Mechanics and Bituminous Materials Research Laboratory, Report No. TE-65-11, University of California, Berkeley, California, (November, 1965).

10 Yettram, Alan L., and Husain, Husain M., "Grid-Framework Method for Plates in Flexure," Journal of the Engineering Mechanics Division, ASCE Vol. 91, (June, 1965), pp. 53-64.

11. McCormick, C. W., "Plane Stress Analysis," Journal of the Structural Division, ASCE Vol. 89, (August, 1963), pp. 37-54.

12. Clough, R. W., "The Finite Element Method in Plane Stress Analysis," Proceedings, 2nd ASCE Conference on Electronic Computation, Pittsburgh, Pa., (Sept., 1960).

MONTANA STATE UNIVERSITY LIBRARIES
3 1762 10013762 7

N378
F868
cop.2
Frazier, G. A.
Analytical investigation of
the vibrational behavior ...

NAME AND ADDRESS
INTERLIBRARY LOAN

N378
F868
cop.2